

# POPULATION SYNTHESIS FOR SYMBIOTIC STARS WITH WHITE DWARF ACCRETORES

Guoliang Lü<sup>1,2,3\*</sup>, L. Yungelson<sup>4</sup> and Z. Han<sup>1</sup>

<sup>1</sup>*National Astronomical Observatories / Yunnan Observatory, the Chinese Academy of Sciences, P.O.Box 110, Kunming, 650011, China*

<sup>2</sup>*Graduate School of the Chinese Academy of Sciences, Beijing, China*

<sup>3</sup>*Department of Physics, Xinjiang University, Ulumqi, 830046, China*

<sup>4</sup>*Institute of Astronomy of the Russian Academy of Sciences, 48 Pyatnitskaya Str., Moscow, Russia*

## ABSTRACT

We have carried out a detailed study of symbiotic stars with white dwarf accretors by means of a population synthesis code. We estimate the total number of symbiotic stars with white dwarf accretors in the Galaxy as 1,200 – 15,000. This range is compatible with observational estimates. Two crucial physical parameters that define the birthrate and number of symbiotic stars are the efficiency of accretion by white dwarfs (which greatly depends on the separation of components after common envelope stage and stellar wind velocity) and the mass of the hydrogen layer which the white dwarf can accumulate prior to the hydrogen ignition. The theoretical estimate of the Galactic occurrence rate of symbiotic novae ranges from about 1.3 to about  $13.5 \text{ yr}^{-1}$ , out of which weak symbiotic novae comprise about 0.5 to  $6.0 \text{ yr}^{-1}$ , depending on the model assumptions. We simulate the distributions of symbiotic stars over orbital periods, masses of components, mass-loss rates of cool components, mass-accretion rates of hot components and luminosity of components. Agreement with observations is reasonable.

**Key words:** binaries: symbiotic — Galaxy: stellar content — accretion — stars: evolution — white dwarf

## 1 INTRODUCTION

Symbiotic stars (SySs) are an inhomogeneous group of variable stars with composite spectra. Their spectacular spectral and photometric variability is a very important and interesting phenomenon. The spectra of SySs suggest that a three-component system consists of a binary system in which an evolved giant transfers matter to a much hotter compact companion by means of stellar wind and an HII region (Berman 1932; Boyarchuk 1967, 1968).

The cool component is a red giant (RG) which is a first giant branch (FGB) or an asymptotic giant branch (AGB) star. In the majority of SySs the hot component is, most probably, a white dwarf (WD), a subdwarf or an accreting low-mass main-sequence (MS) star (Tutukov & Yungelson 1976; Kenyon & Webbink 1984; Mürset et al. 1991; Yungelson et al. 1995, hereafter YLTK; Iben & Tutukov 1996). The variability of SySs may be due to the thermonuclear runaways on the surface of an accreting WD (Tutukov & Yungelson 1976; YLTK; Iben & Tutukov 1996) or to the variations in the accretion rate onto the hot component (Duschl 1986; Bisikalo et al. 2002; Mitsumoto et al. 2005). Recent reviews of the properties

of SySs can be found in Mürset & Schmid (1999) and Mikolajewska (2003). The nova-like eruptions of SySs were reviewed by Mikolajewska & Kenyon (1992).

In astrophysics today, the interaction between components in the binaries is of special interest, for which SySs offer an exciting laboratory (Kenyon 1986). For instance, the nature of components' interaction and of the activity of WD accretors are still controversial (Mürset & Schmid 1999); mass loss and stellar wind (including the terminal velocity and acceleration mechanism) from a cool giant are not clear; SySs have been frequently discussed as Type Ia supernovae progenitors (Tutukov & Yungelson 1976; Munari & Renzini 1992; Kenyon et al. 1993; YLTK; Iben & Tutukov 1996; Hachisu et al. 1999), but their contribution to the rate of these events remains uncertain.

Theoretical studies on the formation and evolution of the SySs have been published, e.g., by YLTK, Han et al. (1995a); Iben & Tutukov (1996); Hurley et al. (2002). Their investigations reproduced successfully many observed properties of these objects. However, in the recent years, a number of papers have appeared that provide new insights in the different aspects of stellar evolution relevant to the SySs. Prialnik & Kovetz (1995) and Yaron et al. (2005) did a more detailed study of Novae models; Nelemans et al. (2000) and Nelemans & Tout (2005) put forward an alternative algo-

\* E-mail: ytlgl@yahoo.com.cn (LGL)

rithm for angular momentum loss during the common-envelope stages of evolution; Winters and his collaborators (Winters et al. 2000, 2002, 2003) studied the hydrodynamical structure of the stellar wind around AGB stars with low mass-loss rate and low wind outflow velocity. New observational catalogue and an analysis of SySs have been given in Belczyński et al. (2000) and Mikołajewska (2003). It is time for a new study of the SySs.

In the present work we model the subpopulation of SySs with WDs as the hot components and FGB or AGB stars as the cool components. We study evolutionary channels leading to the formation of symbiotic systems in which He, CO or ONe WDs accrete hydrogen-rich matter from the stellar wind of FGB or AGB stars. We obtain SySs' birthrate, lifetime and number in the Galaxy, and some potentially observable parameters of SySs, such as orbital periods, masses of the components, their luminosities and mass-loss rates. Special attention is paid to the dependence of population model on the parameters entering population synthesis. This paper is the first one of a series of papers on SySs. It offers a basis for further studies of symbiotic stars, such as D-SySs which are SySs with thick dust shells (paper in preparation).

In § 2 we present our assumptions and describe some details of the modeling algorithm. In § 3 we discuss the main results and the effects of different parameters. In § 4 the main conclusions are given.

## 2 MODELS

In SySs, the cool component loses matter at a high rate by stellar wind and the hot component moves in the wind and accretes enough matter to produce symbiotic phenomenon. In this paper, binaries are considered as SySs if they satisfy the following conditions: (i) The systems are detached; (ii) The luminosity of the hot component is larger than  $10L_\odot$  which is the “threshold” luminosity for the hot component of SySs as inferred by Mikołajewska & Kenyon (1992), Mürset et al. (1991) and YLTK; it may be due to the thermonuclear burning (including novae outbursts, stationary burning and post-eruption burning) or the liberation of gravitational energy by the accreted matter; (iii) The hot component is a WD and the cool component is a FGB or an AGB star. Below we describe our selection algorithm and give some details that are important for understanding the model. All estimates made in the paper are for stars with  $X=0.7$  and  $Z=0.02$ . Chandrasekhar mass limit is taken as  $1.44 M_\odot$ .

### 2.1 Formation Channels of Symbiotic Stars

All progenitors of SySs pass through one of the three routes (YLTK): (i) unstable Roche lobe overflow (RLOF) with formation of a common envelope; (ii) stable RLOF; (iii) formation of a white dwarf+giant pair without RLOF. These scenarios are shown in Fig. 1.

Through channel I pass the systems with short orbital periods. The primary overflows its Roche lobe in the FGB or AGB stage and forms a common envelope. After ejecting the common envelope, it transforms into a WD.

In channel II, the systems undergo stable RLOF. In this

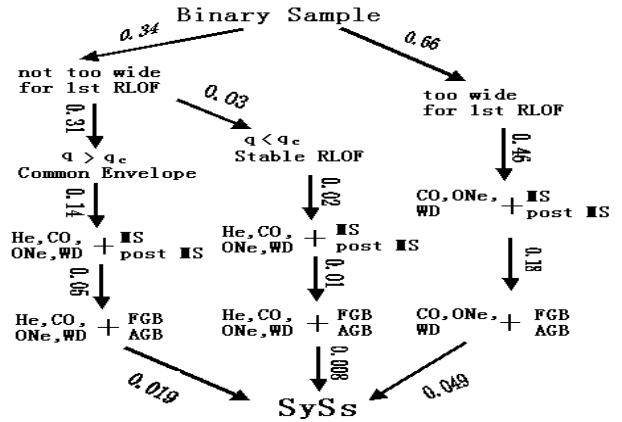


**Figure 1.** —Evolutionary channels for formation of SySs. From left to right channels I, II and III, are shown. RLOF stands for the Roche lobe overflow, MS for main sequence, WD for white dwarf, FGB for the first giant branch, AGB for asymptotic giant branch, SySs for symbiotic stars. Numbers represent fractions of the initial sample of binaries that proceed through the consecutive evolutionary stages of each channel for the “standard” case 1 (see Table 2).

channel, the formation of a helium star is possible. If the helium star is hot enough and the matter inflow rate into the circum-binary medium is high enough, then symbiotic phenomenon can arise. However, the number of systems with helium stars is very small compared to the number of systems with white dwarfs (YLTK; Hurley et al. 2002) and we omit them from consideration.

Through channel III go the systems that are initially wide. In these systems only CO WD or ONe WD accretors are formed.

We consider ONe WDs as remnants of AGB stars that still experience non-degenerate carbon ignition, but avoid electron captures on Ne and Mg in the core. We assume after Pols et al. (1998) that for solar metallicity stars the corresponding range of masses is  $6.1 - 7.9 M_\odot$ . However, the range of masses of ONe WD progenitors still remains uncertain and it may be shifted to higher masses and be much more narrow, several  $0.1 M_\odot$  only (Iben & Tutukov 1985; Gil-Pons & García-Berro 2001, 2002; Gil-Pons et al. 2003; Siess 2006). It is possible that we overestimate the number of systems with ONe WD and, more generally, **initial-final mass relation of Pols et al. (1998) is too steep**.

### 2.2 Common Envelope Evolution

In channels I and II, the primary can overflow its Roche lobe. If the mass ratio of the components ( $q = M_{\text{donor}}/M_{\text{accretor}}$ ) at the onset of RLOF is larger than a certain critical value  $q_c$ , the mass transfer is dynamically unstable and results in the formation of a common envelope. The issue of the criterion for dynamically unstable RLOF  $q_c$  is still open. Hjellming & Webbink (1987) did a detailed study of stability of mass transfer using polytropic models. Han et al. (2001, 2002) showed that  $q_c$  depends heavily on the as-

sumed mass-transfer efficiency. In this work, we adopt  $q_c$  after Hurley et al. (2002):

$$q_c = \left[ 1.67 - x + 2 \left( \frac{M_c}{M} \right)^5 \right] / 2.13, \quad (1)$$

where  $M_c$  and  $M$  are core mass and total mass of the donor, respectively and  $x = 0.3$  is the exponent of the mass-radius relation at constant luminosity for giant stars (Hurley et al. 2000).

For the common envelope evolution, it is generally assumed that the orbital energy of the binary is used to expel the envelope of the donor with an efficiency  $\alpha_{ce}$ :

$$E_{\text{bind}} = \alpha_{ce} \Delta E_{\text{orb}}, \quad (2)$$

where  $E_{\text{bind}}$  is the total binding energy of the envelope and  $\Delta E_{\text{orb}}$  is the orbital energy released in the spiral-in. In the present paper we apply Eq. (2) in the form suggested by Webbink (1984) with modifications after de Kool (1990):

$$\frac{G(M_c + M_e)M_e}{\lambda R_1} = \alpha_{ce} \left( \frac{GM_c m}{2a_f} - \frac{GMm}{2a_i} \right). \quad (3)$$

Here  $\lambda$  is a structure parameter that depends on the evolutionary stage of the donor,  $a_i$  is the orbital separation at the onset of the common envelope,  $M$ ,  $M_c$ , and  $M_e$  are the masses of the donor, donor's envelope and the core, respectively,  $R_1$  is donor's radius and  $m$  is the companion mass. Then the orbital separation of a binary after common envelope phase  $a_f$  is given by

$$\frac{a_f}{a_i} = \frac{M_c}{M} \left( 1 + \frac{2M_e a_i}{\alpha_{ce} \lambda m R_1} \right)^{-1}. \quad (4)$$

Nelemans et al. (2000) suggested to describe the variation of the separation of components in the common envelopes by an algorithm based on the equation for the system orbital angular momentum balance which implicitly assumes the conservation of energy:

$$\frac{\Delta J}{J} = \gamma \frac{M_e}{M + m}, \quad (5)$$

where  $J$  is the total angular momentum and  $\Delta J$  is the change of the total angular momentum during common envelope phase. The orbital separation  $a_f$  after common envelope phase is then

$$\frac{a_f}{a_i} = \left( \frac{M}{M_c} \right)^2 \left( \frac{M_c + m}{M + m} \right) \left( 1 - \gamma \frac{M_e}{M + m} \right)^2. \quad (6)$$

In the runs computed with Eq. (6) we apply it irrespective of the mass ratio of components, as suggested by Nelemans & Tout (2005).

Following Nelemans & Tout (2005) we call the formalism of Eq. (2)  $\alpha$ -algorithm and that of Eq. (5)  $\gamma$ -algorithm. For  $\alpha$ -algorithm, there are two parameters:  $\alpha_{ce}$  and  $\lambda$ . Both parameters are highly uncertain. It's still not completely clear whether sources other than gravitational energy have to be taken into account when computing  $\alpha_{ce}$  and  $\lambda$  and how the core-envelope boundary for the estimate of  $\lambda$  has to be defined (see, e. g., Han et al. 1995b; Iben & Livio 1993; Dewi & Tauris 2000; Tauris & Dewi 2001; Soker & Harpaz 2003). Both parameters depend on the evolutionary stage in which RLOF occurs. In the absence of prescriptions for determination of  $\alpha_{ce}$  and  $\lambda$  for particular donor+accretor combinations one can consider the "combined" parameter

$\alpha_{ce}\lambda$  only. We make computations for  $\alpha_{ce}\lambda=0.5$ , 1.5, and 2.5. The choice of  $\alpha_{ce}\lambda > 1$  is also motivated by the fact that YLTK considered a formulation of the common envelope equation which gives for  $a_f/a_i$  values that are different from the ones given by Eq. (4) and is equivalent to the usage of  $\alpha_{ce}\lambda > 1$  in Eq. (4). Thus, we test both the influence of the uncertainties in the definitions of  $\alpha_{ce}$  and  $\lambda$  and in the formulation of the common-envelope equation.

Generally, we make numerical simulations for the  $\alpha$ -algorithm, but we also check the  $\gamma$ -algorithm effects on the formation of SySs, see Tables 1 and 2. For  $\gamma$ , we consider two values – 1.5 and 1.75 (Nelemans & Tout 2005). For both algorithms we assume that companion mass does not change during common envelope phase since this stage is very short.

### 2.3 The Model of Symbiotic Stars

In SySs, the cool component is in FGB or AGB stage. Because in the core He burning stage the radius and luminosity of the cool component are lower and it can offer very little mass by stellar wind for the hot component accretor, this stage does not contribute to the total population of SySs (YLTK). We therefore skip this stage in our work.

#### 2.3.1 Mass Loss

No comprehensive theory of mass loss for AGB stars exists at present. In this paper, we accept the prescription of Hurley et al. (2000). In MS, Hertzsprung Gap and FGB stages, we apply Reimers (1975) mass-loss law

$$\dot{M}(M_{\odot}\text{yr}^{-1}) = 4 \times 10^{-13} \frac{\eta LR}{M}, \quad (7)$$

where  $\eta = 0.5$  and  $L$ ,  $R$  and  $M$  are the luminosity, radius and mass of the star in solar units, respectively. In AGB stage, we use the mass-loss law suggested by Vassiliadis & Wood (1993)

$$\log_{10}(\dot{M}) = -11.4 + 0.0123(P - 100 \max(M/M_{\odot} - 2.5, 0.0)), \quad (8)$$

where  $P$  is the Mira pulsation period in days given by

$$\log_{10}(P) = -2.07 + 1.94 \log_{10}(R/R_{\odot}) - 0.90 \log_{10}(M/M_{\odot}). \quad (9)$$

When  $P \geq 500$  days, the steady super-wind phase is modeled by the law

$$\dot{M}(M_{\odot}\text{yr}^{-1}) = 2.06 \times 10^{-8} \frac{L/L_{\odot}}{v_{\infty}}, \quad (10)$$

where  $v_{\infty}$  is the terminal velocity of the super-wind in  $\text{km s}^{-1}$ ; we use  $v_{\infty}=15 \text{ km s}^{-1}$  in this paper.

If a star loses mass by stellar wind, it loses angular momentum too. We assume that the lost matter takes away the specific angular momentum of the prospective donor. In this work, the tidal enhancement of mass loss (Tout & Eggleton 1988) is not considered.

For giant-star accretors we assume that the accretion rate is unlimited, since the stars with deep convective envelopes may shrink in the dynamical time scale in response to the mass increase. For non-WD accretors accretion rate is limited by the thermal time scale:  $\dot{M}_2 \leq M_2/\tau_{\text{th},2}$ . For larger  $M_2$ , a common envelope forms.

### 2.3.2 Accretion Rate of Stellar Wind

Stellar wind accretion is crucial for the SySs phenomenon. Shima et al. (1985) and Livio et al. (1986) showed that for SySs the classical Bondi & Hoyle (1944) accretion formula for the stellar wind is generally valid. The mean accretion rate is:

$$\dot{M}_{\text{hot}} = \frac{-1}{\sqrt{1-e^2}} \left( \frac{GM_{\text{hot}}}{v_w^2} \right)^2 \frac{\xi_w}{2a^2} \frac{1}{(1+v^2)^{3/2}} \dot{M}_{\text{cool}}, \quad (11)$$

where  $1 \leq \xi_w \leq 2$  is a parameter ( $\xi_w = \frac{3}{2}$  in this work),  $v_w$  is the wind velocity and

$$v^2 = \frac{v_{\text{orb}}^2}{v_w^2}, \quad v_{\text{orb}}^2 = \frac{GM_{\text{t}}}{a}, \quad (12)$$

where  $a$  is the semi-major axis of the ellipse,  $v_{\text{orb}}$  is the orbital velocity and total mass  $M_{\text{t}} = M_{\text{hot}} + M_{\text{cool}}$ .

If a hot component accretes from the stellar wind of a cool component, a fraction of the angular momentum lost by the cool component is transferred into the spin of the hot component. Following Hurley et al. (2002), we assume that the efficiency of the angular momentum transfer is 1.

### 2.3.3 Wind Velocity

Accretion rate of the stellar wind [Eq. (11)], strongly depends on the wind velocity  $v_w$  which is not readily determined. Taking into account the fact that the hot component may be located in the zone of stellar wind acceleration, we assume that the velocity of the stellar wind is related to the terminal wind velocity  $v_{\infty}$ .

YLTK have defined the wind velocity as

$$v_w = \alpha_w v_{\infty}, \quad (13)$$

where  $v_{\infty}$  is the terminal wind velocity and  $\alpha_w$  is approximated by

$$\alpha_w = \frac{0.04(r/R_d)^2}{1 + 0.04(r/R_d)^2}, \quad (14)$$

where  $r$  is the distance from the donor and  $R_d$  is the radius of the donor. Vogel (1991) gave an empirical formula for the SyS EG Andromedae. This velocity law is:

$$\frac{v_w}{v_{\infty}} = \alpha_w = \begin{cases} c_1(r/R_d)^{10} & \text{for } r/R_d \leq 3.75 \\ 1 - e^{-c_2(r/R_d - c_3)} & \text{for } r/R_d > 3.75, \end{cases} \quad (15)$$

where  $c_1, c_2$  and  $c_3$  are  $0.2 \times (3.75)^{-10}$ ,  $\frac{2}{3}$  and 3.42. Below we present results of numerical simulations for the values of  $\alpha_w$  given by Eqs. (14), (15) and for  $\alpha_w = 1$ .

The definition of terminal velocity in the literature is not unique. YLTK take  $v_{\infty}$  as  $v_{\text{esc}}$  which is the surface escape velocity. But, as noted by Harper (1996), the main characteristic of evolved K and early M-giants' cool winds is that their terminal velocities are lower than the surface escape velocity, typically,  $v_{\infty} \leq \frac{1}{2}v_{\text{esc}}$ . Winters et al. (2000) found two dynamically different regimes for the spherical outflows of AGB stars: in the first regime, the terminal wind velocity is in excess of  $5 \text{ km s}^{-1}$  and the mass-loss rate is higher than  $3 \times 10^{-7} M_{\odot} \text{ yr}^{-1}$ ; in the second regime, the terminal wind velocity is smaller than  $5 \text{ km s}^{-1}$  and the mass-loss rate is lower than  $3 \times 10^{-7} M_{\odot} \text{ yr}^{-1}$ . Winters et al. (2003) fitted the relation between mass-loss rates and terminal wind velocities derived from their CO(2-1) observations by

$$\log_{10}(\dot{M}[M_{\odot} \text{ yr}^{-1}]) = -7.40 + \frac{4}{3} \log_{10}(v_{\infty}/\text{km s}^{-1}). \quad (16)$$

This relation is very close to the results of Olofsson et al. (2004). Mass-loss rates can be obtained by Eq. (8) and  $v_{\infty}$  can be calculated from Eq. (16). Winters et al. (2000) showed the radial structure of hydrodynamic velocity for low and high mass-loss rate models. Obviously, Eqs. (14) or (15), which predict the increase of outflow velocity, are not adequate for the low mass-loss rate model. Semi-regular variable L<sup>2</sup> Pup, whose mass-loss rate is lower than  $3 \times 10^{-7} M_{\odot} \text{ yr}^{-1}$  (Winters et al. 2002), is an example: its photospheric material is moving at a velocity of about  $10 \text{ km s}^{-1}$  which is much higher than its terminal wind velocity of several  $\text{km s}^{-1}$ . In the absence of a clear theory of stellar wind generation and behaviour for low-mass giants we make numerical simulations for a range of assumptions on stellar wind.

For FGB stars we consider two cases:

- (a)  $v_{\infty} = \frac{1}{2}v_{\text{esc}}$ ;
- (b)  $v_{\infty} = v_{\text{esc}}$ .

For AGB stars we consider cases (a),(b), and case (c) in which  $v_{\infty}$  is determined as follows:

For mass loss rate higher than  $3 \times 10^{-7} M_{\odot} \text{ yr}^{-1}$ ,  $v_{\infty}$  is determined by Eq. (16). However, Eq. (16) is valid for  $\dot{M}$  close to  $10^{-6} M_{\odot} \text{ yr}^{-1}$ . For higher mass loss rate, Eq. (16) gives too high a  $v_{\infty}$ . Based on the models of Winters et al. (2000), we assume  $v_{\infty} = \min(30 \text{ km s}^{-1}, v_{\infty})$ . Wind velocity is given by Eq. (13), where  $\alpha_w$  is defined by Eq. (14).

For  $\dot{M} \leq 3.0 \times 10^{-7} M_{\odot} \text{ yr}^{-1}$ , we assume that wind velocity decelerates from  $v_{\text{esc}}$  at the stellar surface to  $5 \text{ km s}^{-1}$  at  $r/R_d = 10$ , using an *ad hoc* function:

$$v_w = \begin{cases} \frac{5 \text{ km s}^{-1} - v_{\text{esc}}}{9} (r/R_d) + \frac{10v_{\text{esc}} - 5 \text{ km s}^{-1}}{9} & r \leq 10R_d \\ 5 \text{ km s}^{-1} & r > 10R_d. \end{cases} \quad (17)$$

(d) In addition, a model with the “standard” terminal wind velocity of AGB stars equal to  $15 \text{ km s}^{-1}$  is calculated.

### 2.3.4 Critical Mass-Accretion Rate of WD

Most models for eruptions in SySs with WD accretors involve the nuclear burning of the material accreted by WDs (Mikołajewska & Kenyon 1992). Based on Tutukov & Yungelson (1976) and Paczyński & Rudak (1979), SySs powered by hydrogen burning on the surface of WDs can be divided further into two subgroups: “ordinary” SySs, which are assumed to burn hydrogen steadily if the mass-accretion rate is above a critical rate,  $\dot{M}_{\text{st}}$ , and symbiotic novae (SyNe)<sup>1</sup>, which experience thermonuclear runaways in their surface hydrogen layers if the mass-accretion rate is lower than  $\dot{M}_{\text{st}}$ . In SyNe stage and stable hydrogen burning stage, the luminosity of the hot component due to hydrogen burning is given by the following approximation for the core mass-luminosity relation for cold WDs accreting hydrogen (Iben & Tutukov 1996):

$$L/L_{\odot} \approx 4.6 \times 10^4 (M_{\text{core}}/M_{\odot} - 0.26). \quad (18)$$

For  $\dot{M}_{\text{st}}$ , following YLTK, we use the approximation to the results of Iben & Tutukov (1989) given by

<sup>1</sup> SyNe represents symbiotic nebulae in some literature but symbiotic novae in this paper.

$$\log_{10} \dot{M}_{\text{st}} (M_{\odot} \text{yr}^{-1}) = -9.31 + 4.12 M_{\text{WD}} - 1.42 (M_{\text{WD}})^2, \quad (19)$$

with  $M_{\text{WD}}$  in solar units. For steady burning, if the mass-accretion rate is above a certain critical rate,  $\dot{M}_{\text{cr}}$ , an accreting WD may evolve into a giant (Kenyon 1986) or generate an optically thick wind (Hachisu et al. 1996). Based on the results of Iben & Tutukov (1989), an approximation to  $\dot{M}_{\text{cr}}$  is given by

$$\log_{10} \dot{M}_{\text{cr}} (M_{\odot} \text{yr}^{-1}) = -9.78 + 9.16 M_{\text{WD}} - 8.13 (M_{\text{WD}})^2 + 2.44 (M_{\text{WD}})^3, \quad (20)$$

where  $M_{\text{WD}}$  is in  $M_{\odot}$ . If the mass-accretion rate is higher than  $\dot{M}_{\text{cr}}$ , we assume that the accreted hydrogen burns steadily at the surface of the WD and hydrogen-rich matter is converted into helium at the rate given by Eq. (25) below, while the unprocessed matter is lost from the system as an optically thick wind and takes away specific angular momentum of the accretor. We also made a test run (case 13 in Table 1) assuming that excess matter expands and transforms the WD into a giant.

In addition, if the accretion rate is higher than a certain value, the release of gravitational energy “mimics” steady hydrogen burning. If the luminosity of the WD due to the liberated gravitational potential energy,  $L_{\text{grav}}$ , is larger than  $10L_{\odot}$ , we assumed that the system powered by accretion is in the “symbiotic stage” too.  $L_{\text{grav}}$  (in solar units) is given by

$$L_{\text{grav}} \sim 3.1 \times 10^7 \dot{M}_{\text{acc}} \frac{M_{\text{WD}}}{R_{\text{WD}}}, \quad (21)$$

where  $\dot{M}_{\text{acc}}$  is in  $M_{\odot} \text{yr}^{-1}$ , and  $M_{\text{WD}}$  and  $R_{\text{WD}}$  are the mass and radius of an accreting WD in solar units, respectively. We note also that variations in mass-flow rate may cause optical outbursts that have distinct spectral features (see discussion in Mikołajewska & Kenyon 1992).

### 2.3.5 Critical Ignition Mass

For SyNe a certain amount of matter has to be accumulated prior to the first explosion. Following YLTK we use the “constant pressure” expression for  $\Delta M_{\text{crit}}$  which implies that the ignition occurs when the pressure at the base of the accreted layer rises to a certain limit:

$$\frac{\Delta M_{\text{crit}}^{\text{WD}}}{M_{\odot}} = 2 \times 10^{-6} \left( \frac{M_{\text{WD}}}{R_{\text{WD}}^4} \right)^{-0.8}, \quad (22)$$

where  $R_{\text{WD}}$  is the radius of zero-temperature degenerate objects (Nauenberg 1972):

$$R_{\text{WD}} = 0.0112 R_{\odot} [(M_{\text{WD}}/M_{\text{ch}})^{-2/3} - (M_{\text{WD}}/M_{\text{ch}})^{2/3}]^{1/2} \quad (23)$$

with  $M_{\text{ch}} = 1.433 M_{\odot}$  and  $R_{\odot} = 7 \times 10^{10}$  cm. In fact  $\Delta M_{\text{crit}}^{\text{WD}}$  is a highly sensitive function of the temperature, mass, and accretion rate of a WD, as well as of assumptions on the nature of the mixing process at the base of the accreted layer and actual nuclear abundances in the accretor. Detailed grids of nova models for CO WD-accretors may be found in Prialnik & Kovetz (1995) and Yaron et al. (2005). Eq. (22) agrees with the results of numerical calculations for relatively cold WDs with the temperature  $10^7$  K (Yaron et al. 2005) within a factor of 5, except for the model with a  $1.4 M_{\odot}$  WD and  $\dot{m} = 10^{-7} M_{\odot} \text{yr}^{-1}$ , for which agreement is within a factor of 7. Nelson et al. (2004) gave numer-

ical fits to the critical ignition masses for novae models calculated by Prialnik & Kovetz (1995). We made a run of the code using the fitting formula for relatively cold ( $T \sim 10^7$  K) WD [see Eq. (A1) of Nelson et al. (2004) in which  $\Delta M_{\text{crit}}^{\text{WD}}$  depends on the mass accretion rates and masses of WD accretors]. Its extrapolation to lower mass ( $0.4 M_{\odot}$ ) agrees with the results of numerical calculations [by the same code; Yaron et al. (2005)] to within a factor less than 3. But for the lowest mass-accretion rates ( $10^{-12}, 10^{-12.3} M_{\odot} \text{yr}^{-1}$ ), its errors are larger. Since the systems with such low mass-accretion rates provide only a tiny contribution to the total number of SySs, we use fits for  $10^{-11} M_{\odot} \text{yr}^{-1}$  in this case. Results agree with the ones in Yaron et al. (2005) to within a factor of less than 3.

Because of the complicated dependence of  $\Delta M_{\text{crit}}$  on the input parameters we ran several simulations varying  $\Delta M_{\text{crit}}$ , see Table 1.

Oxygen-neon WDs need to accrete a more massive envelope than the same mass CO WDs before the outbursts begin (José & Hernanz 1998), because of the lower  $^{12}\text{C}$  abundance in the accretor. Using José & Hernanz (1998) data, we roughly assume that  $\Delta M_{\text{crit}}$  for an ONe WD is twice that for the same mass CO WD.

### 2.3.6 Mass-Accumulation Efficiency

The efficiency of mass accumulation by a WD can never be 100%. First, it strongly depends on the strength of symbiotic novae and, second, even steady-burning WDs blow stellar wind. We define the ratio of the mass of burnt hydrogen to the mass of the matter accreted by a WD as  $\alpha_{\text{H}}$ . The strength of a symbiotic nova depends on the mass and mass-accretion rate of the WD. According to Yaron et al. (2005), we roughly define the boundary between strong SyNe and weak SyNe by the mass-accretion rate  $\dot{M}_{\text{ws}}$  (in  $M_{\odot} \text{yr}^{-1}$ ) which is given by

$$\log_{10} \dot{M}_{\text{ws}} = \begin{cases} -11.01 + 6M_{\text{WD}} & \text{for } M_{\text{WD}} \leq 1M_{\odot}; \\ -1.90M_{\text{WD}}^2, & \text{for } M_{\text{WD}} > 1M_{\odot}. \\ -7.0, & \end{cases} \quad (24)$$

For weak SyNe, *i.e.*, mass-accretion rates being between  $\dot{M}_{\text{st}}$  and  $\dot{M}_{\text{ws}}$ , we use an approximation to  $\alpha_{\text{H}}$  based on Fig. 2 in YLTK [also Fig. 16 of Iben & Tutukov (1996)]:

$$\alpha_{\text{H}} = \begin{cases} -4.39 - 1.48 \log_{10} \dot{M}_{\text{acc}} & \text{for } \log_{10} \dot{M}_{\text{acc}} < -6.36; \\ -0.10 (\log_{10} \dot{M}_{\text{acc}})^2, & \\ 11.66 + 4.56 \log_{10} \dot{M}_{\text{acc}} & \text{for } \log_{10} \dot{M}_{\text{acc}} \geq -6.36 \\ +0.45 (\log_{10} \dot{M}_{\text{acc}})^2, & \end{cases} \quad (25)$$

where  $\dot{M}_{\text{acc}}$  is in  $M_{\odot} \text{yr}^{-1}$ .

For strong SyNe, *i.e.*, mass-accretion rates lower than  $\dot{M}_{\text{ws}}$ , most of the accreted matter is expelled and in some cases even an erosion of the WD occurs (Prialnik & Kovetz 1995; Yaron et al. 2005). Using data on the ejected mass,  $M_{\text{ej}}$ , helium mass fraction in the ejecta,  $Y_{\text{ej}}$ , and in the convective envelope,  $Y_{\text{env}}$ , heavy element mass fraction in the envelope,  $Z_{\text{ej}}$ , and in the ejecta,  $Z_{\text{ej}}$ , given in Table 2 of Yaron et al. (2005), the mass of the burnt hydrogen can be roughly calculated as:

for  $\Delta M_{\text{crit}} \geq M_{\text{ej}}$ ,

$$\Delta M_{\text{H}} = \Delta M_{\text{crit}} \times X_{\text{H}} - M_{\text{ej}} (1 - Y_{\text{ej}} - Z_{\text{ej}}) - (\Delta M_{\text{crit}} - M_{\text{ej}}) (1 - Y_{\text{env}} - Z_{\text{env}}), \quad (26)$$

where we assume that the mixing of the accreted layer with core material does not occur;

for  $\Delta M_{\text{crit}} < M_{\text{ej}}$ , the amount of hydrogen burnt during an outburst is approximated by the difference between  $Y_{\text{env}}$  and  $Y_{\text{ej}}$  which may be computed using data from Prialnik & Kovetz (1995),

$$\Delta M_{\text{H}} = \Delta M_{\text{crit}} Y_{\text{env}} - M_{\text{ej}} Y_{\text{ej}}. \quad (27)$$

Then, using data from Yaron et al. (2005), we fit  $\alpha_{\text{H}}$  by

$$\begin{aligned} \alpha_{\text{H}} &= \frac{\Delta M_{\text{H}}}{\Delta M_{\text{crit}}} \\ &= -0.1391 + 0.7548 M_{\text{WD}} \\ &\quad - 1.0124 M_{\text{WD}}^2 + 0.4739 M_{\text{WD}}^3, \end{aligned} \quad (28)$$

with  $M_{\text{WD}}$  in  $M_{\odot}$ .

For  $\alpha_{\text{H}}$ , if the difference between  $M_{\text{crit}}$  and  $M_{\text{ej}}$  is neglected and the greatest part of the energy released in the outburst is used to lift the ejected shell from the gravitational potential well of the WD, then, according to Yaron et al. (2005), we can give a rough analytical estimate:

$$\alpha_{\text{H}} \approx 4.54 \times 10^{-4} \frac{M_{\text{WD}}}{R_{\text{WD}}}, \quad (29)$$

where  $M_{\text{WD}}$  is the mass of the WD accretor and  $R_{\text{WD}}$  is its radius in solar units.  $\alpha_{\text{H}}$  in Eq. (28) agrees with that in Eq. (29) within a factor of 3 for  $0.4M_{\odot} \leq M_{\text{WD}} \leq 1.4M_{\odot}$  and the former is usually larger than the latter for a given  $M_{\text{WD}}$ .

After a nova, SySs spend certain time in the “plateau” stage with high luminosity. This stage lasts for

$$t_{\text{on}} = 6.9 \times 10^{10} \frac{\alpha_{\text{H}} \Delta M_{\text{crit}}^{\text{WD}}}{L} \text{ yr}, \quad (30)$$

where  $L$  is given by Eq. (18). Stably burning hydrogen “ordinary” SySs are always in the “plateau” stage, their  $\alpha_{\text{H}}$  is given by Eq. (25). In this work the stage of hydrogen burning is denoted as “on”-stage.

For weak SyNe and stable hydrogen burning, we assume that the burnt hydrogen is deposited at the surface of the WD and that the unprocessed matter is lost from the system by the stellar wind that takes away specific angular momentum of the WD. For strong SyNe, the mass of the WD increases if  $M_{\text{ej}} < \Delta M_{\text{crit}}$ . If  $M_{\text{ej}} > \Delta M_{\text{crit}}$ , the WD is eroded. We fit the Yaron et al. (2005) data by a formula

$$\begin{aligned} \frac{M_{\text{ej}}}{\Delta M_{\text{crit}}} &= -28.4700 - 9.6207 \log_{10} \dot{M}_{\text{acc}} \\ &\quad - 1.0372 (\log_{10} \dot{M}_{\text{acc}})^2 - 0.0371 (\log_{10} \dot{M}_{\text{acc}})^3, \end{aligned} \quad (31)$$

where  $\dot{M}_{\text{acc}}$  is in  $M_{\odot} \text{yr}^{-1}$  and which agrees with numerical results to within a factor of 1.4.

### 2.3.7 Decline of SyNe

After the outburst, the system remains observable as a SyS for a time span  $t_{\text{cool}}$ , until the WD cools to the temperature at which its luminosity becomes lower than  $10L_{\odot}$ . Prialnik (1986) showed that the luminosity declines with time as  $L \propto t^{-1.14}$ . Somers & Naylor (1999) confirmed that the observed cooling rate of the WD is consistent with the model of Prialnik (1986). Accordingly, we assume that after “plateau” stage the WD enters decline stage during which its luminosity decreases as

$$L(t) = L(0)t^{-1.14}, \quad (32)$$

where  $L(0)$  is given by Eq. (18) and  $t$  is in years. When  $L(t) = 10L_{\odot}$ , SyS stage terminates and the cooling time  $t_{\text{cool}}$  can be obtained. The lifetime of a SyS is the sum of  $t_{\text{on}}$  and  $t_{\text{cool}}$ .

We assume that during the outburst WD does not accrete any matter, due to the high-velocity wind and high luminosity. At the onset of decline, WD begins to accrete matter from the stellar wind of the cool giant. At the same time, the WD loses mass due to intense radiatively-driven stellar wind (YLTK; Iben & Tutukov 1996). We roughly assume that the rate of the mass loss may be estimated by

$$\dot{M} = \frac{L}{v_{\text{esc}} c}, \quad (33)$$

where  $c$  is the speed of light,  $v_{\text{esc}}$  is escape velocity and  $L$  is the luminosity of the WD given by Eq. (32). In Eq. (33),  $v_{\text{esc}}$  is given by

$$v_{\text{esc}} = \left( \frac{2GM_{\text{WD}}}{R_{\text{WD}}} \right)^{1/2}. \quad (34)$$

In Eq. (34),  $R_{\text{WD}}$  is roughly taken as the radius of a cool WD. The mass-loss rate given by Eq. (33) is uncertain by a factor of several, since during the main part of the “on”-stage the actual radius of the WD is by about an order of magnitude larger than the radius of a cool WD (see, e.g., Mürset et al. 1991; Mürset & Nussbaumer 1994) and the performance number of the radiative stellar wind,  $Mv_{\text{esc}}/(L/c)$ , is not known.

Before the luminosity of the WD declines to  $10L_{\odot}$ , the decline stage may be terminated if the amount of accreted matter is larger than the critical ignition mass.

### 2.3.8 Helium Flashes

When the helium shell accumulates up to a critical mass, the helium flash occurs. This critical mass is about  $(0.1 - 0.2) M_{\odot}$  [for initially cold and non-rotating WDs and  $M \lesssim 3 \times 10^{-8} M_{\odot} \text{yr}^{-1}$ ; e.g., Iben & Tutukov (1991); Woosley & Weaver (1994)]. After a hydrogen flash, the WD becomes “hot” and the helium flashes require ignition mass which is much lower than the above-mentioned critical mass. For hot white dwarfs we use an approximation for the critical mass suggested by Iben & Tutukov (1989, 1996)

$$\Delta M_{\text{crit}}^{\text{He}} = 10^{6.65} R_{\text{WD}}^{3.75} M_{\text{WD}}^{-0.3} \dot{M}_{-8}^{-0.57}, \quad (35)$$

where  $\dot{M}_{-8}$  is the accretion rate in units of  $10^{-8} M_{\odot} \text{yr}^{-1}$  and the remaining variables are in solar units. But Eq. (35) is not valid for the helium accumulation rate lower than  $10^{-8} M_{\odot} \text{yr}^{-1}$ . We take the critical mass for helium ignition as  $0.1 M_{\odot}$  when the helium accumulation rate is lower than  $10^{-8} M_{\odot} \text{yr}^{-1}$ . Mass accumulation efficiency in the helium shell flashes, for a wide grid of masses and accretion rates, is computed by Kato & Hachisu (2004). We find the growth rate of white dwarfs by linear interpolation in these grids. We should note, however, that if white-dwarf accretors are rapid rotators, the helium accumulation efficiency at low  $\dot{M}$  may strongly reduce due to the dissipation of energy at the base of the accreted layer (Yoon & Langer 2004).

## 2.4 Conversion to Observed Parameters

To compare our results with observations, we convert luminosities of cool components into absolute magnitudes using bolometric corrections which can be obtained by interpolation in the BaSeL-2.0 stellar spectra library of Lejeune et al. (1997, 1998). SySs are usually detected due to the presence of features typical for ionized nebulae in the spectra of cool components. This allows us to assume that the simplest selection effect that governs the observed sample of SySs is the visual magnitude of the cool components,  $V_c$  (YLTK). Inspection of the catalogue of SySs (Belczyński et al. 2000) reveals that the number of objects per unit interval of stellar magnitude increases up to  $V_c \sim 12.0$  mag. In both Kenyon (1986) and Belczyński et al. (2000), there are about 50 SySs with  $V_c \leq 12.0$  mag. So, we take 12.0 mag as the limiting stellar magnitude of the complete sample and compute the number of model objects with  $V_c \leq 12.0$  mag.

The number of stars within the distance  $d$  from the Sun is taken to be (Eggleton et al. 1989; Han et al. 1995a)

$$N(d, t) = \frac{1}{d_0^2 t_{\text{Gal}}} \frac{d^3}{\sqrt{d^2 + h^2}}, \quad (36)$$

where  $t$  is the evolutionary age of the star,  $h = 1200(t/t_{\text{Gal}})^{1/2}$  and  $t_{\text{Gal}}$  is the Galactic age. The quantity  $d_0$  is defined such that  $1/\pi d_0^2$  is the density per unit area in the Galactic plane of stars in the solar neighborhood projected onto the plane; following Eggleton et al. (1989), we take  $d_0 = 0.054$  pc and  $t_{\text{Gal}} = 12$  Gyr. Eggleton et al. (1989) used the distance  $d \leq 3$  kpc, we roughly extrapolate  $d$  to 15 kpc in this work for comparison with observations.

To estimate interstellar extinction, we use the corrected relation from van Herk (1965)

$$A_V = 0.14 \times \csc |b| [1 - \exp(-10d \sin |b|)] \text{ mag.}, \quad (37)$$

where  $b$  is the galactic latitude and  $d$  the distance in kpc. Kenyon (1986) showed that Galactic SySs strongly concentrate toward the plane. We roughly take stellar extinction as 1.4 mag per kpc which is the maximum value based on Eq. (37).

## 2.5 Basic Parameters of the Monte Carlo Simulation

For the population synthesis for binary stars, the main input model parameters are: (i) the initial mass function (IMF) of the primaries; (ii) the mass-ratio distribution of the binaries; (iii) the distribution of orbital separations; (iv) the eccentricity distribution; (v) the metallicity  $Z$  of the binary systems.

A simple approximation to the IMF of Miller & Scalo (1979) is used. The primary mass is generated using the formula suggested by Eggleton et al. (1989)

$$M_1 = \frac{0.19X}{(1-X)^{0.75} + 0.032(1-X)^{0.25}}, \quad (38)$$

where  $X$  is a random variable uniformly distributed in the range  $[0,1]$ , and  $M_1$  is the primary mass from  $0.8M_\odot$  to  $8M_\odot$ .

The mass-ratio distribution is quite controversial. We consider only a constant mass-ratio distribution (Mazeh et al. 1992; Goldberg & Mazeh 1994),

$$n(q) = 1, \quad 0 < q \leq 1, \quad (39)$$

where  $q = M_2/M_1$ .

The distribution of separations is given by

$$\log a = 5X + 1, \quad (40)$$

where  $X$  is a random variable uniformly distributed in the range  $[0,1]$  and  $a$  is in  $R_\odot$ .

We assume that all binaries have initially circular orbits. We follow the evolution of both components by the rapid binary evolution code, including the effect of tides on binary evolution (Hurley et al. 2002). We take  $2 \times 10^5$  initial binary systems for each simulation. Since we present, for every simulation, the results of one run of the code, the numbers given are subject to Poisson noise. For simulations with  $2 \times 10^5$  binaries, the relative errors of the numbers of symbiotic systems of different kinds are lower than 7%, with exception of SySs with He WD accretors in cases 6, 10 and 11 (see Table 2). Under model assumptions for cases 6, 10 and 11, SySs with He WD accretors hardly form and the numbers of them expected in the Galaxy are so small (much less than 1 see Table 2) that it is impossible to observe them. We have made a control run for case 10 with a sample of  $6 \times 10^5$  binary systems. The maximum difference among the results obtained for  $2 \times 10^5$  and  $6 \times 10^5$  samples is less than 7% of the numbers presented in Table 2, except for the results on SySs with He WD accretors which agree with the numbers given in columns 2, 10, 14 and 22 of Table 2 within a factor about 2. However, systems with He-accretors constitute only a minor fraction of the total SySs population in case 10 and, hence, inaccuracy in their number has a negligible effect upon our main results. Thus,  $2 \times 10^5$  initial binaries appear to be an acceptable sample for our study.

To calculate the birthrate of SySs, we assume that one binary with  $M_1 \geq 0.8M_\odot$  is formed annually in the Galaxy (Yungelson et al. 1993; Han et al. 1995a; YLTK).

## 3 RESULTS

We construct a set of models in which we vary different input parameters relevant to the symbiotic phenomenon produced by hydrogen burning at the surface of WD accretors. Table 1 lists all cases considered in the present work. case 1\* is considered as the standard model. In addition to the nuclear-burning powered model, we consider an “accretion model” that contains systems in which, under the assumptions of case 1, the liberation of gravitational potential energy produces symbiotic phenomenon ( $L_{\text{grav}} \geq 10L_\odot$ ) before the first outburst of nuclear burning occurs or in the time intervals between consecutive nuclear outburst plus decline “quasi-cycles”.

### 3.1 The history of a typical symbiotic binary

Our main results concerning the numbers of SySs and occurrence rates of SyNe are given in Table 2. But before we discuss them, we present an evolutionary “history” of the typical binary that becomes a SyS (Fig. 2). In this system the initial masses of the primary and the secondary are  $1.2M_\odot$  and  $1.0M_\odot$  and their initial separation is  $1000R_\odot$ . We evolve this binary under conditions appropriate to the

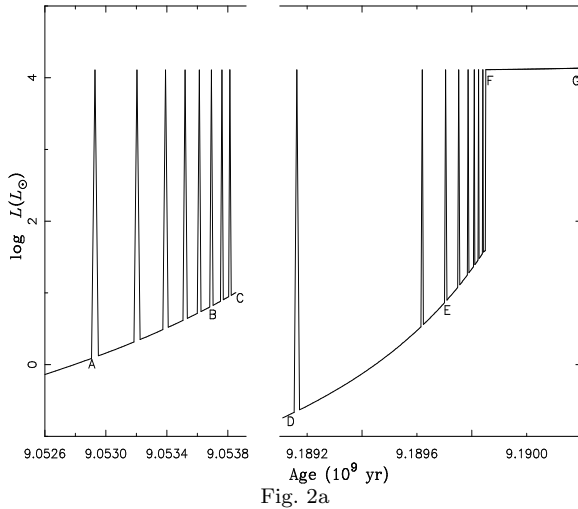


Fig. 2a

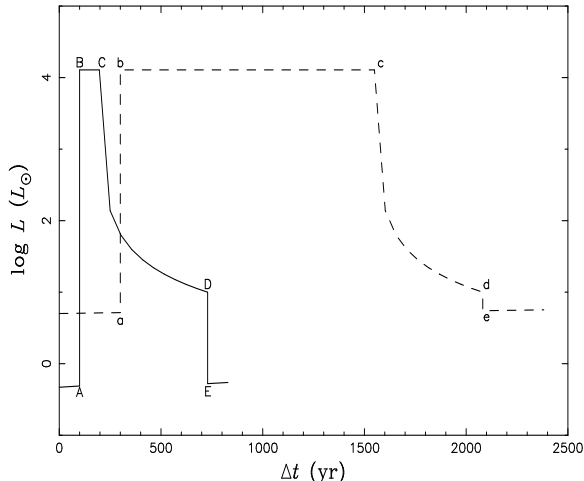


Fig. 2b

**Figure 2.** —Luminosity of the primary component vs. evolutionary age in the system with initial masses of components 1.2 and 1.0  $M_{\odot}$ . Panel *a* represents the evolutionary “history” of the system as a SyS. Panel *b* shows the details of luminosity evolution during the first strong and weak novae experienced by the system (solid and dashed lines, respectively). See text for details.

**Table 1.** Parameters of the models of the population of symbiotic stars. Case 1\* means the standard model. In case 6,  $v_{\infty}$  of FGB stars is taken as  $v_{\text{esc}}$  and it is  $\frac{1}{2}v_{\text{esc}}$  in other cases. In case 7, wind velocity  $v_w$  is treated as described under item (c) in subsection 2.3.3. In case 13, critical ignition mass is taken after Eq. (A1) from Nelson et al. (2004).

case	Common envelope	$v(\infty)$	$\alpha_w$	$\Delta M_{\text{crit}}^{\text{WD}}$	Optically thick wind
case 1*	$\alpha_{\text{ce}}\lambda = 0.5$	$\frac{1}{2}v_{\text{esc}}$	Eq. (13)	$\Delta M_{\text{crit}}^{\text{WD}}$	on
case 2.	$\alpha_{\text{ce}}\lambda = 1.5$	$\frac{1}{2}v_{\text{esc}}$	Eq. (13)	$\Delta M_{\text{crit}}^{\text{WD}}$	on
case 3.	$\alpha_{\text{ce}}\lambda = 2.5$	$\frac{1}{2}v_{\text{esc}}$	Eq. (13)	$\Delta M_{\text{crit}}^{\text{WD}}$	on
case 4.	$\gamma = 1.5$	$\frac{1}{2}v_{\text{esc}}$	Eq. (13)	$\Delta M_{\text{crit}}^{\text{WD}}$	on
case 5.	$\gamma = 1.75$	$\frac{1}{2}v_{\text{esc}}$	Eq. (13)	$\Delta M_{\text{crit}}^{\text{WD}}$	on
case 6.	$\alpha_{\text{ce}}\lambda = 0.5$	$v_{\text{esc}}$	Eq. (13)	$\Delta M_{\text{crit}}^{\text{WD}}$	on
case 7.	$\alpha_{\text{ce}}\lambda = 0.5$	Eq. (16)	Eq. (13)	$\Delta M_{\text{crit}}^{\text{WD}}$	on
case 8.	$\alpha_{\text{ce}}\lambda = 0.5$	$15 \text{ km s}^{-1}$	Eq. (13)	$\Delta M_{\text{crit}}^{\text{WD}}$	on
case 9.	$\alpha_{\text{ce}}\lambda = 0.5$	$\frac{1}{2}v_{\text{esc}}$	Eq. (14)	$\Delta M_{\text{crit}}^{\text{WD}}$	on
case 10.	$\alpha_{\text{ce}}\lambda = 0.5$	$\frac{1}{2}v_{\text{esc}}$	1	$\Delta M_{\text{crit}}^{\text{WD}}$	on
case 11.	$\alpha_{\text{ce}}\lambda = 0.5$	$\frac{1}{2}v_{\text{esc}}$	Eq. (13)	$3\Delta M_{\text{crit}}^{\text{WD}}$	on
case 12.	$\alpha_{\text{ce}}\lambda = 0.5$	$\frac{1}{2}v_{\text{esc}}$	Eq. (13)	$\frac{1}{3}\Delta M_{\text{crit}}^{\text{WD}}$	on
case 13.	$\alpha_{\text{ce}}\lambda = 0.5$	$\frac{1}{2}v_{\text{esc}}$	Eq. (13)	$*\Delta M_{\text{crit}}^{\text{WD}}$	on
case 14.	$\alpha_{\text{ce}}\lambda = 0.5$	$\frac{1}{2}v_{\text{esc}}$	Eq. (13)	$\Delta M_{\text{crit}}^{\text{WD}}$	off

“standard” case 1\*. When the system attains point A in Fig. 2a, the primary has become a CO WD of  $M = 0.54M_{\odot}$ , the secondary is in the FGB stage, the system still is not a SyS. At point A, the first strong symbiotic nova occurs and the system becomes a SyS. After the first strong symbiotic nova, the system leaves the state of being a SyS, while accretion onto the WD continues until the next symbiotic nova occurs. Before reaching point B, the system undergoes 5 strong SyNe. As the mass accretion rate increases, accretor enters the regime of weak thermonuclear runaways at point

B (in the latter regime no erosion of WD is expected, see § 2.3.6). The system experiences 3 weak SyNe, before the secondary leaves the FGB stage at point C. After return to the giant branch but before reaching point D, the secondary is an AGB star but the system does not manifest itself as SySs. At point D, a strong symbiotic nova occurs. After two strong SyNe, the system begins to undergo weak symbiotic novae at point E. After 6 weak SyNe, the system enters the stage of steady hydrogen-burning by the accretor at point F. At point G, the secondary overflows its Roche lobe and the system leaves SySs’ stage. After the 4th outburst in the D-F stage in Fig 2, in the inter-outburst time intervals, the star contributes to the accretion model, since its  $L$  never drops below  $10L_{\odot}$ .

Figure 2b shows in detail the evolution of the luminosity during the first strong and weak novae experienced by the system. At point A (a), the outburst occurs and the luminosity rapidly increases. From points B (b) to C (c), the system is in the “plateau” stage. From points C (c) to D (d), the system is in the decline stage. At point D(d) the luminosity of the accretor drops below  $10L_{\odot}$  and we no longer consider the system as a SyS, since its accretion luminosity (represented by point E(e)) does not satisfy the criterion for SySs. Accretion continues until critical ignition mass of hydrogen is accumulated again. Figure 2b also shows that the “on”-stage for the weak novae is much longer than that for the strong ones.

### 3.2 Birthrate and number of SySs

First, we discuss the gross properties of the modeled population of SyS and then proceed to the more detailed comparison of the influence of different assumptions. As Table 2 shows, the Galactic birthrate of SySs may range from about 0.035 (case 6) to 0.131 (case 4)  $\text{yr}^{-1}$  and it is about 0.076  $\text{yr}^{-1}$  in the standard model. Their number is from about 1,200 (case 6) to 15,100 (case 4) and it is close to 4,300 in the standard model. The contribution of SySs with He WD accretors to the total number of SySs is negligible, due to

**Table 2.** Different models of symbiotic stars population. The first column gives model number according to Table 1. Columns 2 to 8 give the birthrates of SySs with accretors of different kinds (He-, CO- or ONe WD), the rate of SySs formation through evolutionary channels I, II, and III (Fig. 1) and total birthrate. The ratio of the number of SySs in cooling stage and their total number is given in column 9. Columns 10 to 13 give the occurrence rates of SyNe with accretors of different kinds (He-, CO- or ONe-WD) and total rate, in the 13th column the numbers in parentheses mean the rates of weak SyNe. Total Galactic number of SySs with accretors of different kinds (He-, CO- or ONe-WD), the number of SySs formed through evolutionary channels I, II, and III and total number are shown in columns 14 to 20, respectively. The 21st column gives the total numbers of Galactic SySs with cool components having apparent visual magnitude  $\leq 12.0$ . Columns 22 to 25 give the numbers for SyNe with accretors of different kinds (He-, CO- or ONe-WD) that are currently in the “plateau” stage of an outburst and their total number, in the 25th column the number in parentheses means the number of weak SyNe.

Model	Birthrate of SySs( $\text{yr}^{-1}$ )							$\frac{N_{\text{cooling}}}{N_{\text{total}}}$	Occurrence Rate of SyNe ( $\text{yr}^{-1}$ )			
	He	CO	ONe	I	II	III	total		He	CO	ONe	total
1	2	3	4	5	6	7	8	9	10	11	12	13
Standard	0.001	0.070	0.005	0.019	0.008	0.049	0.076	0.32	0.002	1.4	2.0	3.4 (1.5)
Accretion	0.0	0.045	0.004	0.001	0.008	0.040	0.049	—	—	—	—	—
case 2	0.004	0.080	0.006	0.033	0.008	0.049	0.090	0.38	0.012	1.8	2.3	4.1 (1.7)
case 3	0.006	0.086	0.007	0.041	0.008	0.049	0.098	0.41	0.022	2.1	2.6	4.7 (1.8)
case 4	0.018	0.106	0.006	0.074	0.008	0.049	0.131	0.33	0.160	6.9	6.4	13.5 (6.0)
case 5	0.014	0.099	0.007	0.062	0.008	0.049	0.119	0.34	0.120	3.9	5.1	9.2 (3.7)
case 6	0.0001	0.032	0.003	0.007	0.005	0.023	0.035	0.46	0.0001	1.1	0.6	1.7 (0.9)
case 7	0.001	0.121	0.007	0.019	0.008	0.102	0.129	0.62	0.002	5.5	6.5	11.9 (2.8)
case 8	0.001	0.078	0.006	0.014	0.004	0.067	0.085	0.59	0.002	1.8	4.1	5.9 (2.4)
case 9	0.003	0.074	0.005	0.026	0.006	0.050	0.082	0.26	0.007	1.0	1.8	2.8 (1.3)
case 10	0.00001	0.061	0.005	0.003	0.003	0.060	0.066	0.45	0.00001	0.9	2.5	3.4 (1.9)
case 11	0.0002	0.047	0.005	0.010	0.008	0.034	0.052	0.17	0.0002	0.4	0.8	1.3 (0.5)
case 12	0.004	0.089	0.006	0.027	0.008	0.064	0.099	0.52	0.011	4.3	4.5	8.8 (4.0)
case 13	0.001	0.071	0.005	0.016	0.008	0.053	0.077	0.46	0.001	4.8	4.6	9.5 (5.7)
case 14	0.001	0.070	0.005	0.019	0.008	0.049	0.076	0.37	0.002	1.4	1.8	3.2 (1.4)

—continue

Model	Number of SySs							Number of SySs ( $V_c \leq 12.0$ )	Number of SyNe			
	He	CO	ONe	I	II	III	total		He	CO	ONe	total
1	14	15	16	17	18	19	20	21	22	23	24	25
Standard	$\leq 1$	3860	420	250	2280	1750	4300	19	$\leq 1$	407	5	412 (393)
Accretion	0	6870	170	230	3730	3090	7100	37	—	—	—	—
case 2	10	4220	570	780	2280	1750	4800	23	3	471	5	480 (450)
case 3	20	4610	690	1290	2280	1750	5300	32	10	563	6	580 (543)
case 4	2060	11910	1080	11070	2280	1750	15100	73	599	1306	15	1920 (1858)
case 5	820	9260	1120	7180	2280	1750	11200	59	304	1114	13	1432 (1380)
case 6	$\leq 1$	1130	90	50	780	380	1200	4	$\leq 1$	103	1	105 (99)
case 7	$\leq 1$	8830	2470	190	1680	9430	11300	74	$\leq 1$	1242	9	1251 (1167)
case 8	$\leq 1$	2770	920	140	700	2860	3700	23	$\leq 1$	301	7	309 (280)
case 9	$\leq 4$	3280	320	230	2120	1260	3600	12	$\leq 1$	197	4	201 (182)
case 10	$\leq 1$	1600	360	30	340	1580	2000	6	$\leq 1$	146	5	151 (140)
case 11	$\leq 1$	3220	240	100	1960	1420	3500	13	$\leq 1$	393	5	398 (383)
case 12	5	5360	680	600	2970	2470	6000	32	$\leq 1$	411	4	416 (395)
case 13	$\leq 1$	4980	420	250	2960	2180	5400	26	$\leq 1$	409	4	413 (394)
case 14	$\leq 1$	3290	400	250	2030	1400	3700	21	$\leq 1$	406	5	411 (392)

their large hydrogen ignition mass, except for cases 4 and 5 in which their contribution is respectively close to 14% and 7%; the contribution of SySs with ONe WD accretors strongly depends on assumptions and the ranges from about 7% (case 4) to 25% (case 8); SySs with CO WD accretors contribute the main fraction of the population. Observational estimates of the total number of SySs range from several thousands (Boyarchuk 1970) to about 30,000 (Kenyon 1994) or even up to 300,000 (Munari & Renzini 1992), depending on the assumptions on the distance to a typical SyS and on observational selection.

In the catalogue of Belczyński et al. (2000), there are 52 SySs with  $V_c \leq 12.0$  mag. In some cases  $V_c$  is the magnitude in outburst. In our models, the number of SySs with a cool component brighter than  $V_c = 12.0$  is from 4 (case 6) to 74 (case 7). In the standard model, in combined nuclear

and accretion models, there are in total 56 SySs within this magnitude limit, i.e., about 0.5% of all systems! The situation is similar for simulations with other assumptions. Thus, we may infer that a sample of observed symbiotic stars that may be considered as statistically complete, contains only fractions of a percent of all Galactic SySs.

In the nuclear models, from about 38 (case 7) to 83 (case 11) percent of SySs are in the “on”-state (including stably-burning stars and stars in outbursts) and the rest are in the cooling stage. When an outburst occurs, the hot component spends some time in the “plateau” stage. We assume that the time-span of the “plateau” stage is the lifetime of a SyNe. In total, the fraction of the SyNe currently in the “on”-stage among all SyS (in the outburst and decline stages) varies from about 5% (case 9) to 13% (case 7).

The contribution of SyNe with He WD accretors to the

total number of SyNe is about 31% in case 4 and 21% in case 5 but it is negligible in other cases; due to very short lifetime of outbursts in SyNe with ONe WD accretors, their contribution is also negligible (its range is from approximately 0.4% in case 7 to 2% in case 8); most SyNe have CO WD accretors. In the Galaxy, the model occurrence rate of SyNe is between ranges from about  $1.3 \text{ yr}^{-1}$  (case 11) to  $13.5 \text{ yr}^{-1}$  (case 4). The contribution of SyNe with ONe WD accretors to the total rate is close to 60% in most cases, in extreme cases it is 74% (case 10) and 35% (case 6). The contribution of SyNe with He WD accretors to the total rate of Novae is negligible. Note, the role of systems with ONe accretors is rather uncertain because of uncertainty of their progenitors' range and may be one of the reasons for the relatively high total occurrence rate of SyNe in our models.

### 3.3 Parameters

**1. Common Envelope Evolution:**  $\alpha$ -algorithm — In the cases 2 and 3, the parameter  $\alpha_{ce}\lambda$  is increased from 0.5 to 1.5 and 2.5, respectively. The larger  $\alpha_{ce}\lambda$  is, the more easily the common envelope is ejected, then the orbital period of a binary system after common envelope phase is longer, which is favourable for the formation of SySs. The occurrence rate of SyNe and the total number of SySs in cases 2 and 3 become larger than in the standard model. On  $\alpha_{ce}\lambda$  depends only formation channel I (Fig. 1) in which the common envelope is encountered. The number of systems produced through this channel increases with  $\alpha_{ce}\lambda$  since more systems avoid merger in common envelopes. The number of SySs and the occurrence rate of SyNe change with increased  $\alpha_{ce}\lambda$  by the same proportion as the birthrate in channel I, since the outbursts are associated predominantly with relatively more massive dwarfs which are produced mainly through channels II and III.

**2. Common Envelope Evolution:**  $\gamma$ -algorithm — In case 5,  $\gamma$  is increased to 1.75 from 1.5 in case 4. Based on Eq. (5), the larger  $\gamma$  is, the smaller the separation of the binary is after the common envelope phase  $a_f$  (since more orbital angular momentum is taken from the system). The birthrate of SySs having undergone channel I in case 5 is lower than that in case 4, but  $\gamma$ 's effect is weak.

However, there is great difference between  $\alpha$ -algorithm cases (1, 2 and 3) and  $\gamma$ -algorithm cases (4 and 5). The birthrate of SySs formed through channel I in case 4 is about 3.9 times of that in the standard model, the birthrate of SySs with He WD accretors in case 4 is about 18 times of that in the standard model, and the total birthrate of SySs in case 4 is 1.7 times higher than that in the standard model. The occurrence rate of SyNe and the total number of SySs in case 4 are much larger than those in the standard model. The reason is that with  $\gamma$ -algorithm post-common-envelope systems are wider than with  $\alpha$ -algorithm and this facilitates symbiotic phenomenon, allowing more stars to evolve further along FGB or AGB before the second RLOF. The  $\gamma$ -mechanism is especially favourable for a larger fraction of SySs with He-WD accretors among all SyS since it (i) allows the progenitors of He-WDs to avoid merger, (ii) hydrogen shells accreted by He-WDs are more massive, while their luminosity is lower, hence, they live as SySs longer. Also, in case 4 more massive white dwarfs survive common envelopes

and this results in a sharp increase in the occurrence rate of SyNe.

**3. Parameter  $v_\infty$**  — The comparison of cases 1, 6, 7 and 8 shows that  $v_\infty$  is a key factor for forming SySs. For a given mass loss rate, the decrease of  $v_\infty$  increases the efficiency of accretion, facilitating SyS formation. This is best exemplified by comparison of cases 1 and 6. In case 7 in early AGB stage, the accretion efficiency of a WD is enhanced due to low  $v_\infty$ , but the mass loss rate of a cool giant is not high. In late AGB stage, the mass loss rate of a cool giant is high, but the accretion efficiency of a WD is low due to rapidly rising  $v_\infty$ . As a result of these effects, the rate of accretion onto WDs stays in the range which is favourable for the occurrence of SyNe (see Fig. 8 and Table 2).

**4. Parameter  $\alpha_w$ :** — In case 9, the wind velocity law suggested by Vogel (1991) is adopted. This empirical law gives very low velocities in the vicinity of the cool component, which results in more efficient accretion and hence increases birthrate and number for the closest systems with a He-WD, but slightly reduces them for systems with CO- and ONe-WDs. However, for  $\alpha_w = 1$  in case 10 wind velocity in the vicinity of the accretor is high. This strongly decreases the birthrates of SySs formed through channels I and II. Also, SySs with He-WD accretors are hardly formed. For the systems formed through channel III the birthrate and number almost do not depend on  $\alpha_w$ , since for wide systems  $\alpha_w$  is close to 1 for all wind-acceleration laws.

**5. Parameter  $\Delta M_{WD}^{\text{crit}}$**  — In cases 12 and 11,  $\Delta M_{WD}^{\text{crit}}$ , the threshold value for “ignition” of symbiotic novae, are, respectively,  $\frac{1}{3}$  and 3 times of that in the standard model. The occurrence rate of SyNe and total number of SySs rapidly increase from case 11 to the standard model and to case 12, but the numbers of SyNe and SySs in the burning stage are basically invariable, since the amount of hydrogen available for burning is the same in all cases. In case 13, Eq. (A1) of Nelson et al. (2004) is used for  $\Delta M_{WD}^{\text{crit}}$ . Compared with Eq. (22), it agrees within a factor close to 2 when the mass accretion rate is  $10^{-9} M_\odot \text{yr}^{-1}$ . However, Eq. (A1) of Nelson et al. (2004) gives  $\Delta M_{WD}^{\text{crit}}$  that are, on the average, 3 times lower than the ones given by Eq. (22) when the mass accretion rate is  $10^{-8} M_\odot \text{yr}^{-1}$  and 7 times lower when the mass accretion rate is  $10^{-7} M_\odot \text{yr}^{-1}$ . So the occurrence rate of SyNe increases.

**6. Optically thick wind** — Comparing cases 1 and 14, we find that it is practically unimportant for the model of the population of SySs whether there is an optically thick wind or not. SyNe are not affected, since they occur at low  $M$ . In case 14, the total number of SySs decreases because in the absence of optically thick winds expansion of accretors and formation of common envelopes in the highest  $\dot{M}$  systems becomes unavoidable. The outcome of common envelope is either merger of components or formation of a double-degenerate.

To summarize, we find that the assumed formalism for the common envelope evolution, terminal wind velocity and  $\Delta M_{WD}^{\text{crit}}$  have the strongest effect upon the occurrence rate of SyNe and total number of SySs, introducing uncertainty up to factors  $\simeq (3-4)$ . The wind velocity law affects the occurrence rate of SyNe and the number of SySs within factor  $\leq 2$ .

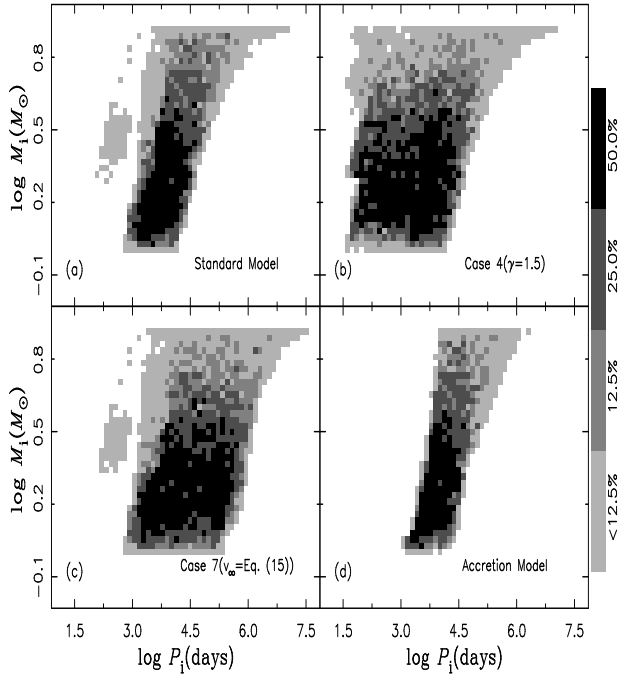


**Figure 3.** —Gray-scale maps of initial primary mass  $M_i$  vs. initial orbital period  $P_i$  distribution for the progenitors of SySs. The gradations of gray-scale correspond to the regions where the number density of systems is, respectively, within  $1 - 1/2$ ,  $1/2 - 1/4$ ,  $1/4 - 1/8$ ,  $1/8 - 0$  of the maximum of  $\frac{\partial^2 N}{\partial \log P_i \partial \log M_i}$ , and blank regions do not contain any stars. The cases shown in particular panels are indicated in their lower right corners.

### 3.4 Properties of SySs

In this section, we describe potentially observable physical quantities of SySs. We compare the standard model ( $\alpha$ -algorithm for common envelope evolution), case 4 ( $\gamma$ -algorithm for common envelope evolution), case 7 (low outflow velocity for AGB stars), and the accretion model.

Figure 3 shows the distributions of the progenitors of SySs, in the “initial primary mass – initial orbital period” plane. Most SySs descend from  $(1.0 - 2.5) M_\odot$  stars, this is an effect of the IMF. The Figure also shows well that for  $\alpha$ -algorithm for common envelopes, in most SySs, accretors form from AGB stars. The distribution  $\log M_i - \log P_i$  in case 4 ( $\gamma=1.5$ ) is different from that in other cases, because for the  $\gamma$ -algorithm, common envelopes result in rather moderate shrinkage of orbits or even in their expansion, allowing relatively close systems to avoid merger, as already noted above. In this case also stars in FGB contribute to the formation of SySs, particularly, by formation of He-WD accretors and relatively low-mass CO-WD accretors, see also Fig. 5 below. The distribution becomes more even in case 7 because under assumption of low  $v_\infty$  in the systems formed through Channel III velocity of the matter passing by WD is lower than in the “standard” case and accretion becomes more efficient. For the “accretion” model the distribution has more narrow range of periods since, in fact, the objects of this model, are a subsample of standard model which had  $L > 10 L_\odot$  prior to the first outburst or between outbursts.

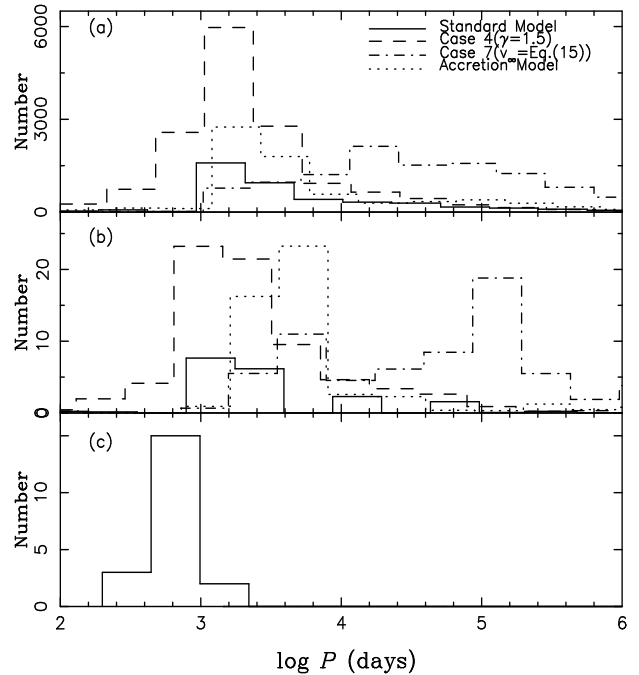


**Figure 4.** —Number distributions of SySs as a function of orbital periods. Panel *a* shows distributions in total samples for standard model, accretion model and cases 4, and 7, while panel *b* shows distribution for a sub-sample with cool components brighter than  $V_c = 12.0$  mag. See the key to lines in panel *a*. In panel *c* observational data from Mikolajewska (2003) and Belczyński et al. (2000) is plotted.

#### 3.4.1 Orbital Periods

Figure 4 shows the distributions of SyS over orbital periods. The plot for the total sample, panel *a*, shows that in case 4 ( $\gamma$ -algorithm) the distribution is wider than in the standard case ( $\alpha$ -algorithm) since in the former case there are systems which avoided merger and retained or even increased their initial separations. In case 7, there are more SySs with long orbital periods than in the standard case thanks to the systems that form through Channel III and manifest symbiotic phenomenon because of the low wind velocity which enhances accretion efficiency.

The distribution of observed SyS with  $V \leq 12.0$  mag. over orbital periods based on the data from Belczyński et al. (2000) and Mikolajewska (2003) is plotted in Fig. 4c. It may be compared with the distributions for the model subsamples of systems with  $V \leq 12.0$  mag. (Fig. 4b). The overwhelming majority of case 1 and case 4 model systems with  $V < 12$  in Fig. 4b are almost uniformly distributed between 1000 and 6000. However, orbital periods are measured for less than 30 systems out of almost 200 known SySs and it is hard to measure long orbital periods. The predictions of models about orbital period can be hardly verified. However, Fig. 4 suggests that SySs with orbital periods shorter than 200 day are hardly expected, which is in agreement with observations.

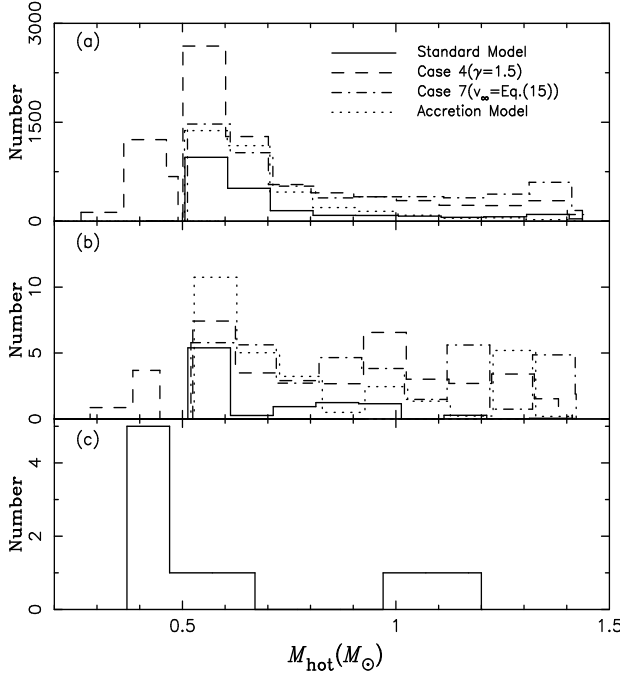


**Figure 5.** —Number distributions of model Galactic SySs as a function of the hot component mass. Fig. 5a is for the total samples, Fig. 5b is for a sub-sample with cool components brighter than  $V_c = 12.0$  mag, and Fig. 5c is plotted based on the data in Mikolajewska (2003) and Belczyński et al. (2000). The key to the line-styles representing different models is given in the upper right corner of Fig. 5a.

### 3.4.2 Properties of Hot Components

In Fig. 5, the distributions of the masses of hot components are shown. The distribution for case 4 ( $\gamma=1.5$ ) is different from other cases. In case 4, there is a peak between approximately  $0.35$  and  $0.5 M_\odot$  which represents the distribution of masses of He WD accretors. Note, the masses of these dwarfs are close to the upper limit of the masses of He WDs. In other cases, the contribution of SySs with He WD accretors is negligible. For all nuclear models, the distributions have peaks around  $0.6 M_\odot$  and a slight enhancement by  $1.35 M_\odot$ . The peak is due to the distribution of CO WD masses. The enhancement at the tail of the distribution is due to the massive WD accretors (especially ONe WDs) that undergo many outbursts because of low hydrogen ignition mass. The model distribution for the sub-sample for SySs with cool components brighter than  $12.0$  mag. is shown in Fig. 5b. The distribution of the estimated masses of hot components in systems with  $V_c \leq 12.0$  mag. [as given in Belczyński et al. (2000) and Mikolajewska (2003)], is plotted in Fig. 5c. Though it is still small number statistics, we should note that only with the  $\gamma$ -formalism for common envelopes is it possible to obtain the prominent fraction of low-mass accretors which is present in the observed population. Note the presence of relatively massive WD-accretors also in the observed population, though not so prominent as in case 7 and not extending to the range of masses of ONe WDs. The excess of massive WDs, if real, may be a counterargument to the case 4 model.

Figure 6 presents, in gray scale, the relation between

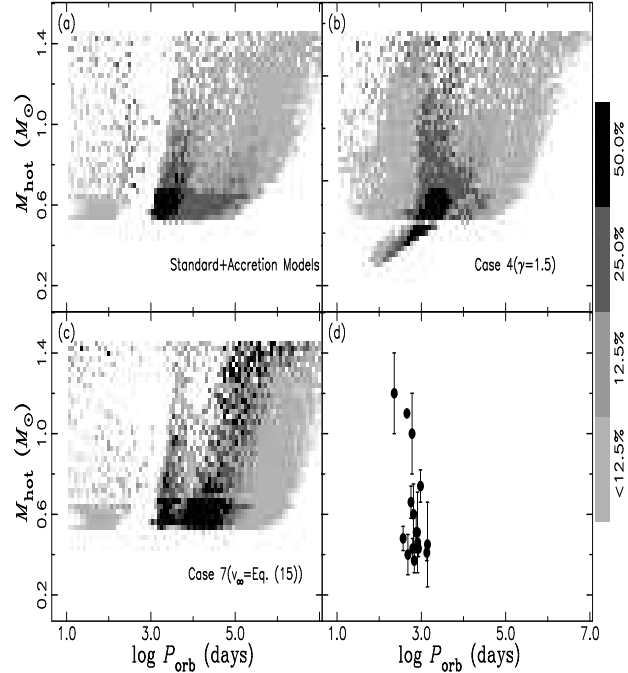


**Figure 6.** —Gray-scale maps of the model distributions of the masses of hot components vs. orbital periods. The gradations of gray-scale correspond to the regions where the number density of systems is, respectively, within  $1 - 1/2$ ,  $1/2 - 1/4$ ,  $1/4 - 1/8$ ,  $1/8 - 0$  of the maximum of  $\frac{\partial^2 N}{\partial \log P_{\text{orb}} \partial \log M_{\text{hot}}}$ , and blank regions do not contain any stars. Fig. 6d is based on the data for observed systems from Mikolajewska (2003).

the masses of the hot components and orbital periods of SyS. The distributions in Figs. 6a and c, are split into two domains. The scarcely populated left one represents SySs formed through channel I; the right domain is populated by systems formed through channels II and III. The gap between the two domains is absent in case 4 in which systems that went through channel I did not experience a sharp decrease of orbital separation. Panel c shows that a low velocity stellar wind favours symbiotic phenomenon in systems within a wider range of orbital separations than in the models with high velocity.

The comparison with observed systems shows that our models correctly predict that the majority of hot components of SySs must have masses around  $(0.5-0.6) M_\odot$ , though the existence of some lower mass (He-WD) accretors cannot be excluded. Note that mass estimates typically assume orbital inclinations of  $i = 90^\circ$  or a limit to  $i$  (see Table 2 in Mikolajewska (2003)), hence, the estimates are lower limits. Orbital periods of the systems with measured  $M_{\text{hot}}$  are also consistent with theoretical expectations. At the same time our models suggest the existence of a significant number of SyS with yet unmeasured periods larger than 1000 day.

Panel 6d shows that there is a group of “outliers” – systems with relatively short periods and massive accretors. Among them is the prominent recurrent nova system T CrB ( $P \approx 227.6$  day,  $M_{\text{hot}} = 1.2 \pm 0.2 M_\odot$ ,  $M_{\text{cool}} = 0.7 \pm 0.2 M_\odot$ ). Progenitors of such systems must have high initial mass primaries and be sufficiently wide to form a massive WD and have large initial mass-ratios of components to enable

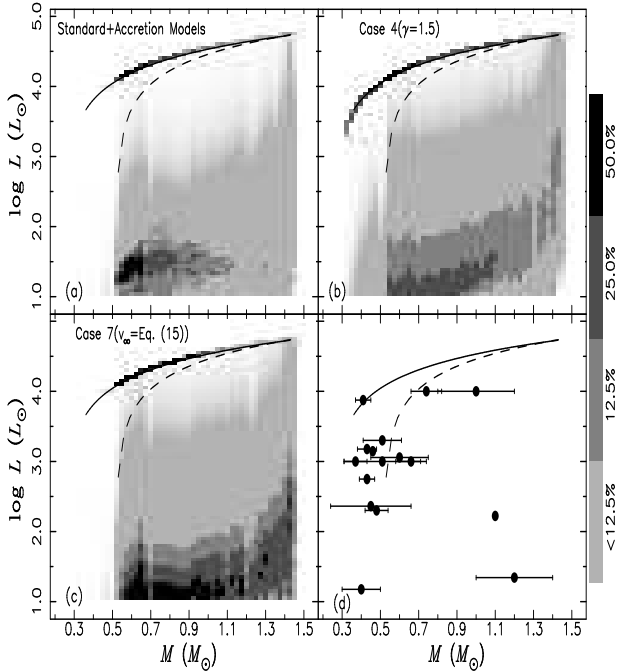


**Figure 7.** —Gray-scale maps of the distribution of luminosities of hot components in SySs vs. their masses. The gradations of gray-scale correspond to the regions where the number density of systems is, respectively, within  $1 - 1/2$ ,  $1/2 - 1/4$ ,  $1/4 - 1/8$ ,  $1/8 - 0$  of the maximum of  $\frac{\partial^2 N}{\partial \log L \partial \log M}$ , and blank regions do not contain any stars. Fig. 7d shows  $M_{\text{hot}}$  estimates from Mikołajewska (2003). Solid line shows relation between mass of accreting WD and its luminosity (18), dashed line is (Paczynski 1970; Uus 1970) mass-luminosity relation for AGB stars  $L/L_{\odot} = 6.0 \times 10^4(M_c/M_{\odot} - 0.52)$ .

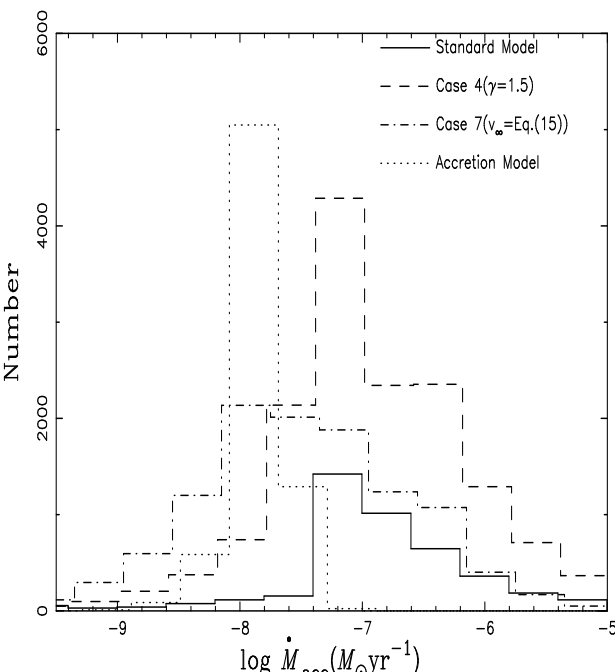


**Figure 8.** —Number distributions of model SySs as a function of the mass-accretion rate of the hot components.

**Table 3.** An example of an evolutionary scenario leading to formation of T CrB-like system. Masses are in  $M_{\odot}$ ,  $P_{\text{orb}}$  in days. The values of binary parameters at the onset of respective stage are given.

	MS,MS	AGB,MS	CE	WD,MS	WD,FGB	CE
$M_1$	7.09	6.83	2.19	1.28	1.28	1.28
$M_2$	0.90	0.90	1.25	1.25	1.25	1.19
$P_{\text{orb}}$	7817	8155	10622	277	277	263

sufficient shrinkage of the orbit in common-envelope event. With the notation already used above, we present a numerical example for formation and evolution of a system that may belong to this group (in the standard model) in Table 3. The system manifests symbiotic phenomenon in the “WD,FGB”-stage. The giant loses only about  $0.06M_{\odot}$  of the matter before RLOF and the WD experiences about 1500 strong Novae (this number is rather uncertain because of the uncertainty in  $\Delta M_{\text{crit}}^{\text{WD}}$ ). Note, the mass of WD practically does not change.

Figure 7 shows the relations between orbital periods of SyS and the luminosities of their hot components. By our definition of SySs, there are 3 states of WDs in them, see § 3.1 and Fig. 2. Steady-burning systems and SyNe systems in the plateau stage obey the mass-luminosity relation (18). These systems are located in Fig. 7 along the solid line representing Eq. (18). Then, when they are in the decline stage, they deviate from (18) downward. Stars in the plateau and decline stages form the upper populated area in Fig. 7a,b,c. Next, as Fig. 2 shows, stars rapidly transit into an “accretion” stage where they spend time comparable or even longer than in the “nuclear-burning” stages. This explains the formation of the lower populated domain in Fig. 7 and the existence of a gap between the two regions. The lower cut-off at  $L/L_{\odot} = 10$  corresponds to our definition of SySs as systems with a larger luminosity WD. The difference in the density of systems in different regions of Fig. 7a,b,c may be understood as a consequence of different period distributions and accretion efficiencies in different cases. This picture is reasonably consistent with observations plotted in Fig. 7d which shows that most observed systems are in the decline stage, but, probably, observational selection favours detection of the brightest systems only<sup>2</sup>. Stars in the long accretion stage are not observed because of their low luminosities. Because hot components of the observed systems in the mass-luminosity plot are located between Iben-Tutukov and Paczynski-Uus curves but not below the latter curve, Fig. 7d also suggests that mass-luminosity relation for *hydrogen-accreting* WDs is really close to Iben-Tutukov relation (18) and differs from Paczynski-Uus relation  $L/L_{\odot} = 6 \times 10^4(M_c/M_{\odot} - 0.52)$  which describes the luminosity of *AGB stars with double nuclear-burning shells*.

In Fig. 8, the distributions of mass accretion rates onto the hot components  $\dot{M}_{\text{acc}}$  are shown. For all nuclear models the distributions have peaks close to  $10^{-7} M_{\odot} \text{ yr}^{-1}$ ; for the

<sup>2</sup> Iben & Tutukov (1996) also suggest that observed symbiotic stars are in the stage when their luminosity is provided by residual nuclear burning and cooling luminosity of WD.

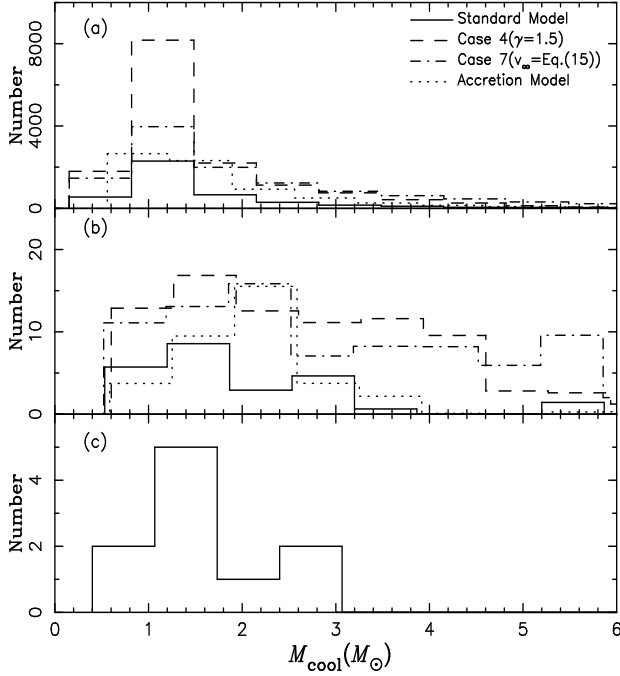


**Figure 9.** —Number distributions of model SySs as a function of the mass of the cool components. Panel a is for the total samples, panel b is for a sub-samples with cool components brighter than  $V_c = 12.0$  mag and panel c presents data from Belczyński et al. (2000) and Mikołajewska (2003).

accretion model the peak is close to  $10^{-8} M_\odot \text{ yr}^{-1}$ . The first peak and its extension to the larger  $L$  correspond to the rate of stable hydrogen burning at the surface of typical WD accretors, while the second peak corresponds to the release of  $10L_\odot$  by accretion.

During an outburst, the hot component may support an additional high-velocity wind [e.g., Kenyon (1986); Iben & Tutukov (1996)]. As noted by the latter authors, wind mass-loss may shorten the lifetime of SyS in the “on”-state. Another related effect is the formation of a temporary “common envelope” by an extended envelope of the white dwarf during outburst and associated mass loss. We neglect here these two effects. Note, collision of the winds from components is important for the formation of observational features of SySs, but it does not influence their evolution.

### 3.4.3 Properties of Cool Components

The cool component supplies the matter accreted by the hot one. The mass of the cool component gradually decreases. In Fig. 9a, the distributions of cool components’ masses are shown. In all cases, the great majority of masses are confined to the range  $(0.8 - 2.0) M_\odot$ . The distributions for the model sub-samples with cool components brighter than  $V_c = 12.0$  mag are shown in Fig. 9b, the distribution of the masses of observed cool components of SySs with  $V_c \leq 12.0$  mag. (Belczyński et al. 2000; Mikołajewska 2003) is plotted in Fig. 9c. Results of our simulations reasonably agree with observations.

Figure 10a shows the distributions of mass ratios of cool components to hot components for the total model samples.

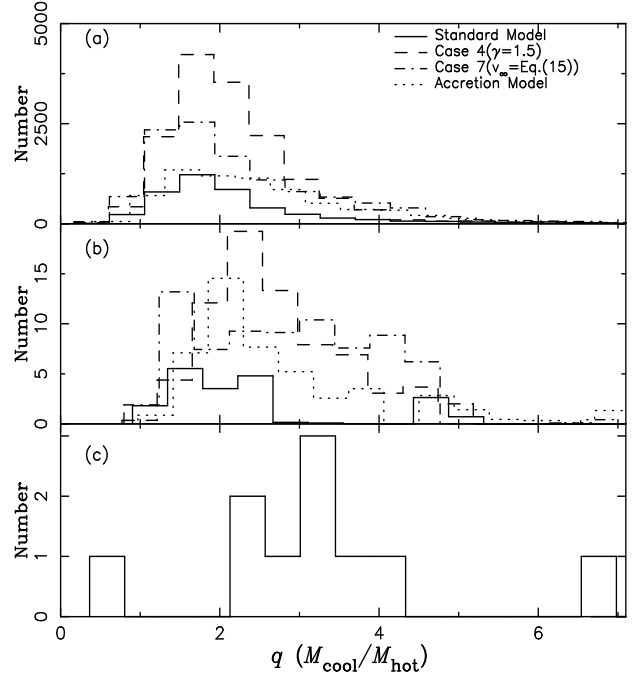


**Figure 10.** —Number distributions of model SySs as a function of the mass ratio of components. Fig. 10a is for the total samples, Fig. 10b is for a sub-sample with cool components brighter than  $V_c = 12.0$  mag., and Fig. 10c presents estimates of  $q$  in observed systems after Belczyński et al. (2000) and Mikołajewska (2003).

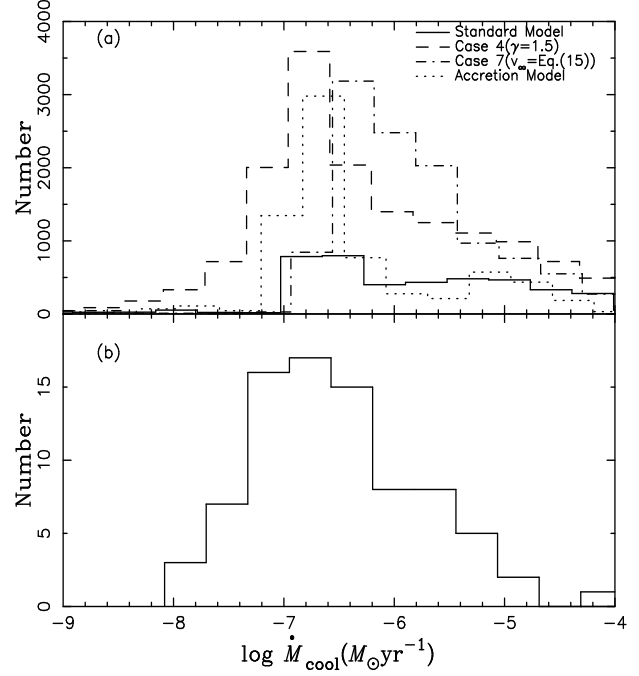


**Figure 11.** —Number distributions of model SySs over mass-loss rate of the cool component. Fig. 11a is for total model samples. Fig. 11b presents the observational data from Seaquist et al. (1993).

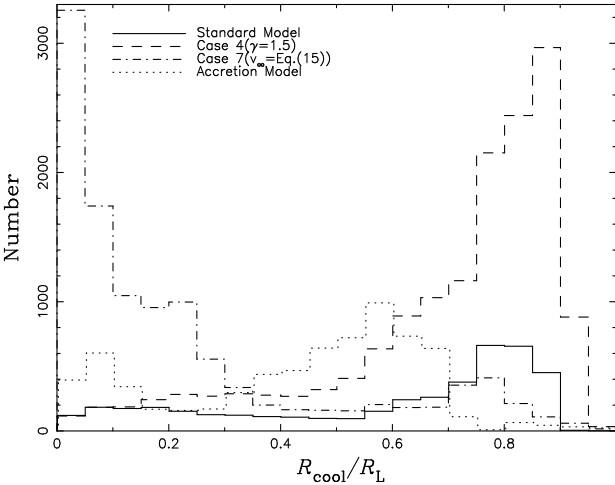


Figure 12. —Number distributions of model SySs over the ratios of donor radius to the Roche lobe radius of cool component.

The distributions for the model sub-samples with cool components brighter than  $V_c = 12.0$  mag. are shown in Fig. 10b. The peaks in Fig. 10a for all cases are close to 1.8. Figure 10c shows the distribution of the observational estimates of  $q$  for systems with  $V_c \leq 12.0$  mag. from Belczyński et al. (2000); Mikolajewska (2003). The peak in Fig. 10b is located between 2 and 4. We do not consider this discrepancy as critical. First, it is based on very small number statistics. Second, the masses for observed cool components are typically assigned based on their spectral types and evolutionary tracks, but for M-giants the masses within the same spectral subtype may differ by a factor larger than 2 (Dumm & Schild 1998).

In Fig. 11, the distributions of SySs over mass-loss rates from the cool components are shown. The peaks in Fig. 11a for the total samples are between  $10^{-7}$  and  $10^{-6} M_\odot \text{yr}^{-1}$ . The observational estimates of the mass-loss rates after Seaquist et al. (1993) are plotted in Fig. 11b. Comparison of Figs. 11a and 11b shows that our results agree reasonably well with observations.

Figure 12 shows the distributions of the cool components over the ratio of their radii to the radii of their Roche lobes. In Fig. 12, the distribution for case 7 is different from other nuclear cases. In case 7, the maximum is below 0.3, but it is between 0.7 and 0.9 in the standard model and case 4. The main reason for the difference is velocity of the stellar wind. In the standard model the rate of mass-loss increases with evolutionary lifetime,  $\alpha_w$  evaluated by Eq. (14) decreases, thus, the model favours symbiotic stars with donors close to the Roche lobe. In case 7, velocity of the stellar wind is low during the early AGB stage and this favours symbiotic stars with relatively compact donors.

Mürset & Schmid (1999) found that M-type giants in symbiotic binaries obey the relation  $R \leq l_1/2$  where  $R$  is the radius of the cool component and  $l_1$  is the distance from the center of the cool component to the inner Lagrangian point  $L_1$ . Note, it is difficult to compare Fig. 12 directly with the observational data because Sp-M, Sp-R relations are not unique for stars in the late stages of their evolution. Mürset & Schmid (1999) applied, for the radii of giants, the median values from Dumm & Schild (1998), although the

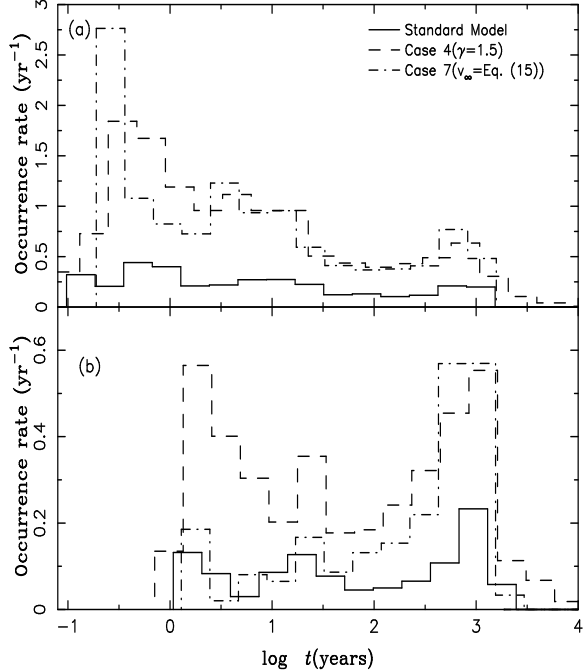


Figure 13. —Occurrence rate of SyNe (Fig. 13a) and weak SyNe (Fig. 13b) as a function of the duration of outbursts.

real radius may be several times different. However, if the pattern found by Mürset & Schmid (1999) is really correct, the model of SySs will require a rather low velocity of stellar wind in the low mass loss rate phase but a high wind velocity in the high mass loss rate phase, which is consistent with the stellar wind model of Winters et al. (2000).

#### 3.4.4 Symbiotic Novae

For the nuclear models, the most important property of SySs is their thermonuclear runaways. The length of the outbursts depends on the mass and mass-accretion rate of the WD-component. As Fig. 13a shows, SyNe last from several months to thousands of years. The distributions in Fig. 13a can be roughly separated into two domains. In the first domain, below 1 yr, there are peaks around 4 months. The first domain corresponds to the strong SyNe. The second domain extends from about 1 yr to several hundred (even several thousand) yr. As Fig. 13b shows, to this domain contribute, predominantly, weak SyNe.

In the standard model for the population of Galactic SyNe, the contribution of weak SyNe to the total occurrence rate of SyNe is approximately 40%; it ranges from 24% in case 7 [ $v_\infty = \text{Eq. (16)}$ ] to 56% in case 10 ( $\alpha_w = 1$ ). If we consider the number of systems experiencing thermonuclear runaways, it appears that, due to the shorter lifetime of strong SyNe, the contribution of systems with weak SyNe to the total number of SyNe-systems is larger than 90%.

Figure 13 shows that some outbursts last for more than 1000 years. These outbursts occur on low-mass He-WDs. This is especially prominent in case 4 ( $\gamma = 1.5$ ) in which a large number of He WD accretors form. However, these long outbursts are more difficult to detect. Observed outbursts last for months to years or for dozens of years (Kenyon 1986;

Mikołajewska 2003). The outburst of AG Peg lasted for 100 years. Thus the double-peak structure of the distribution in Fig. 13a is, crudely, consistent with observations. We suggest the existence of two populations of SySs – those with short outbursts and those with long ones.

Note that the observed flashes of SyNe with small amplitude (1 to 3 mag) may also be due to the variations of mass-transfer rate and/or accretion disk instabilities and associated variations in the nuclear burning rate (Duschl 1986; Bisikalo et al. 2002; Mitsumoto et al. 2005; Sokoloski et al. 2006).

For the occurrence rate of SyNe, Iben & Tutukov (1996), taking into account the fact that four outbursts were observed within 4 kpc from the Sun in the past 25 years, obtained a mean value of  $\nu \sim 3 \text{ yr}^{-1}$ . From the number of SyNe's "fossils", Lewis (1994) estimated the frequency of SyNe as about  $0.4 \text{ yr}^{-1}$ , which may be considered as the lower limit. Our model estimates are between  $1.3 \text{ yr}^{-1}$  and  $13.5 \text{ yr}^{-1}$ . In the standard model, the occurrence rate of SyNe is close to  $3.4 \text{ yr}^{-1}$ , which agrees with Iben & Tutukov (1996) estimates. Comparing our results to the observational estimates, one should note the following: first, not all SyNe are observed; second, it is difficult to confirm the event of SyNe if it lasts for more than 100 yr. The problem of the incompleteness of the sample of Symbiotic Novae was, in fact, never explored.

#### 3.4.5 Symbiotic Stars and Supernovae Ia

All models for Supernovae Ia (SNe Ia) involve accreting WDs. The efficiency of the accumulation of helium shell mass is very important if we consider SySs as the potential progenitors of SNe Ia. Helium flashes may occur in our models because the critical ignition helium mass is very low (See Eq. (35)) when the mass accumulation rate of helium is higher than  $10^{-8} M_\odot \text{ yr}^{-1}$ . The range of their occurrence rate is between about  $0.0006 \text{ yr}^{-1}$  (case 6) and  $0.008 \text{ yr}^{-1}$  (case 4), and the occurrence rate in the standard model is close to  $0.005 \text{ yr}^{-1}$ .

Kenyon et al. (1993), YLTK, Yungelson et al. (1996) and Yungelson et al. (1998) showed that it is unlikely that SySs can produce SN Ia via accumulation of the Chandrasekhar mass. Our results agree with this conclusion. In all cases, the frequency of events in which a CO WD reached the Chandrasekhar limit is lower than  $10^{-6} \text{ yr}^{-1}$ . The reason is the lack of massive accreting CO WDs and the inefficient increase of core masses (Fig. 14) and even erosion of accretors (especially, for massive WD). This is clearly seen from Fig. 14: accumulated helium shell masses do not exceed  $0.1 M_\odot$ .

The low efficiency of helium accumulation also makes symbiotic stars bad candidates for SNe Ia produced by "edge-lit detonation (ELD)" — detonation of core carbon initiated by detonation of accreted helium in WDs in the mass range  $0.6$ – $0.9 M_\odot$ , after accreting  $0.15$ – $0.2 M_\odot$  of He at  $\dot{M} \sim 10^{-8} M_\odot \text{ yr}^{-1}$ . [e.g., (Livne 1990; Limongi & Tornambé 1986; Woosley & Weaver 1994)]. In all our models, the detonation of accreted helium can not occur, that is, there is not a sample in which accumulated helium shell mass exceeds  $0.15 M_\odot$ . We calculated the rate of events in which a  $0.1 M_\odot$  helium shell is accumulated on CO WDs with masses larger than  $0.6 M_\odot$  in all models.

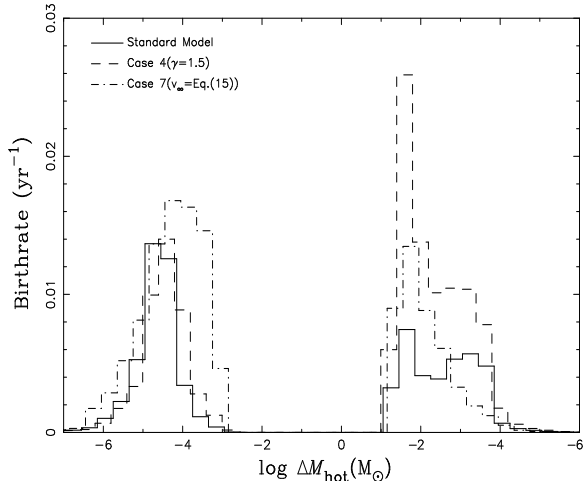


**Figure 14.** — Occurrence rate distributions of SySs as a function of the mass changes of CO WD accretors. The bins to the left of 0 at x-axis show eroding WD, while to the right of 0 – mass-accumulating WD.

This rate is  $< 10^{-5} \text{ yr}^{-1}$ . Furthermore, as we mentioned above, in the case of fast rotation, outbursts of accreted He may occur after accretion of only several  $0.01 M_\odot$  of matter (Yoon & Langer 2004). Then, "Helium Novae" may occur.

#### 3.5 Comparison with YLTK

YLTK performed a detailed population-synthesis study of SySs. In the standard model of YLTK, the estimate of the birthrate of SySs in the Galaxy is  $0.076 \text{ yr}^{-1}$  and their number is close to 3,300, which is similar to our results in the standard model. Certain differences between the models stem from the fact that Eq. (1) takes into account the stabilizing effect of a large mass of stellar core upon RLOF for stars with convective envelopes that was not considered in YLTK.

The main difference with YLTK is the estimate of the birthrate of SySs with He WD accretors. In YLTK it is about  $0.024 \text{ yr}^{-1}$ ; for CO WD accretors it is about  $0.049 \text{ yr}^{-1}$ . Because of difference in lifetimes, the numbers of systems with different accretors are more similar: 1560 and 1740. In the standard model of the present paper, the number of SySs with He WD accretors is negligible. There are two main reasons for this: 1. For the same value of  $\alpha_{ce}$ , the common envelope formalism of Webbink (1984) – Eq. (3), gives larger reduction of component separation than the YLTK model, leaving no room for formation of SySs with He WD accretors. In case 4 ( $\gamma=1.5$ ), the common envelope model gives a smaller reduction of binary separation than Webbink's model, then SySs with He WD accretors appear. 2. In both models, binaries with He WDs form through common envelopes or RLOF from FGB stars. However, in YLTK the upper mass range of the progenitors of He WDs extends to  $2.5 M_\odot$ , while in the present study it is taken as  $2.0 M_\odot$ . This difference also allows additional He-accretor systems to form in simulations of YLTK.

Both studies agree that symbiotic stars are not likely precursors of SN Ia.

## 4 CONCLUSION

We performed a detailed study of the formation of symbiotic systems with WDs as hot components, employing the population synthesis approach to the evolution of binaries. Several important conclusions can be drawn:

1. The number of nuclear symbiotic stars in the Galaxy may range from about 1,200 to 15,000. These numbers are compatible with observational estimates. The model birthrate of SySs in the Galaxy is from 0.035 to 0.131  $\text{yr}^{-1}$ .

2. The estimated occurrence rate of symbiotic Novae is between 1.3  $\text{yr}^{-1}$  and 13.5  $\text{yr}^{-1}$ ; weak SyNe contribute to this rate from about 0.5 to 6.0 events per yr. This estimate greatly depends on the critical ignition mass of the hydrogen shell  $\Delta M_{\text{WD}}^{\text{crit}}$  and accretion efficiency. It may be compared to the estimate of the Galactic occurrence rate of classical Novae  $41 \pm 20 \text{ yr}^{-1}$  (Hatano et al. 1997). It looks likely that the models with high rates of symbiotic novae strongly overestimate this rate. This can mean that (i) the relative fraction of massive accretors is overestimated because of too steep initial-final mass relation; (ii) the values of hydrogen-ignition mass  $\Delta M_{\text{WD}}^{\text{crit}}$  implied by us may be underestimated; (iii) mass loss by stellar winds from accreting dwarfs is underestimated or (iv) accretion efficiency is overestimated. The latter issue has to be resolved by gas-dynamical calculations of mass-flows in symbiotic systems. Note also, that tripling of  $\Delta M_{\text{WD}}^{\text{crit}}$  in case 11 brings occurrence rate of SyNe to about 1 per yr; having in mind the paucity of observed SyNe this low number may be preferred. Ignition masses given by Eq. (22) are typically higher than the masses computed by Prialnik & Kovetz (1995); Yaron et al. (2005). This may mean that the latter studies also strongly underestimate  $\Delta M_{\text{WD}}^{\text{crit}}$ .

There may exist two varieties of symbiotic stars — those with short outbursts and those with long ones.

3. The evolution of symbiotic stars is unlikely to lead to SNe Ia via accumulation of Chandrasekhar-mass or to the edge-lit detonations. Helium novae may occur in symbiotic systems if the energy is efficiently dissipated at the base of accumulated He-layer.

4. The results of the modeling depend on the assumed common-envelopes formalism. Within  $\alpha$ -formalism, variations of combined parameter  $\alpha_{\text{ce}}\lambda$  do not strongly affect model population, since it is dominated by wide systems and systems that experience stable RLOF. Increase of  $\alpha_{\text{ce}}\lambda$  shifts the systems produced via channel I into the ranges of parameters of descendants of channels II and III.

The main effect of applying  $\gamma$ -formalism is the dominance of systems formed through common envelopes. Comparison with observations, whenever possible (Table 2, Figs. 4 – 11), suggests that using  $\gamma$ -formalism it is easier to explain variety of parameters of observed SySs. This especially concerns existence of short-period systems and the tendency of SySs for harbouring relatively low-mass accretors. There is apparent excess of Novae in  $\gamma$ -formalism models. However, this may be also an effect of the underestimate of critical ignition masses or the overestimate of the number of systems with massive accretors.

5. The wind velocity law affects the occurrence rate of SyNe and the number of SySs within a factor of 2. Observational data is still not sufficient to provide real restrictions on the models.

6. To summarize, the models for the population of SySs mostly depend on the assumed formalism for the common envelope evolution and critical mass for hydrogen ignition  $\Delta M_{\text{WD}}^{\text{crit}}$ . These factors have the strongest effect upon the occurrence rate of SyNe and the total number of SySs, introducing an uncertainty up to a factor of about 4.

## ACKNOWLEDGMENTS

We are grateful to the referee, C. Tout, for careful reading of the paper and constructive criticism. We thank Li-fang Li, Xuefei Chen and Xiangcun Meng for some helpful suggestions, and Fenghui Zhang for providing the data on bolometric corrections. We acknowledge J. Mikołajewska for providing us a compilation of orbital periods of symbiotic stars. LGL thanks Dr. Richard Pokorny for correcting English language of the manuscript. This work was supported by Chinese National Science Foundation under Grants Nos. 10433030 and 10521001, the Foundation of the Chinese Academy of Sciences (KJCX2-SW-T06) and Russian Academy of Sciences Basic Research Program “Origin and Evolution of Stars and Galaxies”. LRY acknowledges warm hospitality of the Astronomical Institute “Anton Pannekoek” where a part of this study was done and support from NWO and NOVA.

## REFERENCES

- Belczyński K., Mikołajewska J., Munari U., Ivison R. J., Friedjung M., 2000, A&AS, 146, 407
- Berman L., 1932, PASP, 44, 318.
- Bisikalo D. V., Boyarchuk A. A., Kilpio E. Yu., Kuznetsov O. A., 2002, ARep, 46, 1022
- Bondi H., Hoyle F., 1944, MNRAS, 104, 273
- Boyarchuk A. A., 1967, Soviet Astronomy, 11, 8
- Boyarchuk A. A., 1968, Soviet Astronomy, 11, 818
- Boyarchuk A. A., 1970, in *Eruptivnye Zvezdy*, ed. A. A. Boyarchuk & R. E. Gershberg (Moscow: Nauka), 113
- de Kool M., 1990, ApJ, 358, 189
- Dewi J. D. M., Tauris T. M., 2000, A&A, 360, 2043
- Dumm T., Schild H., 1998, NewA, 3, 137
- Duschl W. J., 1986, A&A, 163, 61
- Eggleton P. P., Fitechett M. J., Tout C. A., 1989, ApJ, 347, 998
- Gil-Pons P., García-Berro E., 2001, A&A, 375, 87
- Gil-Pons P., García-Berro E., 2002, A&A, 396, 589
- Gil-Pons P., García-Berro E., José J., Hernanz M., Truran T. W., 2003, A&A, 407, 1021
- Goldberg D., Mazeh T., 1994, A&A, 282, 801
- Hachisu I., Kato M., Nomoto K., 1996, ApJL, 470, 97
- Hachisu I., Kato M., Nomoto K., 1999, ApJ, 522, 487
- Han Z., Eggleton P. P., Podsiadlowski P., Tout C. A., 1995a, MNRAS, 277, 1443
- Han Z., Podsiadlowski P., Eggleton P. P., 1995b, MNRAS, 272, 800
- Han Z., Eggleton P. P., Podsiadlowski Ph., Tout C. A., Webbink R. F., 2001, ASP Conf. Ser., 229, 205
- Han Z., Podsiadlowski, Ph., Maxted P. F. L., Marsh T. R., Ivanova N., 2002, MNRAS, 336, 449

Harper G., *Cool Stars, Stellar Systems, and the Sun. 9th Cambridge Workshop ASP Conference Series*, Vol.109, 1996, Roberto Pallavicini and Andrea K. Dupree (eds.)

Hatano K., Branch D., Fisher A., Starrfield S., 1997, MNRAS, 290, 113

Hjellming M. S., Webbink R. F., 1987, ApJ, 318, 749

Hurley J. R., Pols O. R., Tout C. A., 2000, MNRAS, 315, 543

Hurley J. R., Tout C. A., Pols R., 2002, MNRAS, 329, 897

Iben I. Jr., Tutukov A. V., 1985, ApJS, 58, 661

Iben I. Jr., Tutukov A. V., 1989, ApJ, 342, 430

Iben I. Jr., Tutukov A. V., 1991, ApJS, 370, 615

Iben I. Jr., Livio M., 1993, PASP, 105, 1373

Iben I. Jr., Tutukov A. V., 1996, ApJS, 105, 145

José J., Hernanz M., 1998, ApJ, 494, 680

Kato M., Hachisu I., 2004, ApJL, 613, 129

Kenyon S. J., Webbink R. F., 1984, ApJ 279, 252

Kenyon S. J., 1986, *The Symbiotic Stars*(Cambridge: Cambridge Univ. Press)

Kenyon S. J., Livio M., Mikołajewska J., Tout C. A., ApJL, 407, 81

Kenyon S. J., 1994, Mem. S.A.It, 65, 135

Lejeune T., Cuisinier F., Buser R., 1997 A&AS, 125, 229

Lejeune T., Cuisinier F., Buser R., 1998 A&AS, 130, 65

Lewis B. M., 1994, A&A, 288, L5

Limongi M., Tornambé A., 1991, ApJ, 371, 317

Livio M., Soker N., de Kool M., Savonije G.M., 1986, MNRAS, 222, 235

Livne E., 1990, ApJL, 354, 53

Mazeh T., Goldberg D., Duquennoy A., Mayor M., 1992, ApJ, 401, 265

Mikołajewska J., Kenyon S. J., 1992, MNRAS, 256, 177

Mikołajewska, J. 2003, Astronomical Society of the Pacific Conference Series, 303, 9

Miller G. E., Scalo J. M., 1979, ApJS, 41, 513

Mitsumoto M., Jahanara B., Matasuda T., et al., 2005, ARep., 49, 884

Munari U., Renzini A., 1992, ApJL, 397, 87

Mürset U., Nussbaumer H., Schmid H. M., Vogel M., 1991, A&A, 248, 458

Mürset U., Nussbaumer H., 1994, A&A, 282, 586

Mürset U., Schmid H. M., 1999, A&A, 137, 473

Nauenberg M., 1972, ApJ, 175, 417

Nelemans G., Verbunt F., Yungelson L. R., Portegies Zwart S. F., 2000, A&A, 360, 1011

Nelemans G., Tout C. A., 2005, MNRAS, 356, 753

Nelson L. A., MacCannell K. A., Dubeau E., 2004, ApJ, 602, 938

Olofsson H., González Delgado D., Kerschbaum F., Schöier F. L., 2002, A&A, 391, 1053

Paczyński B., 1970, Acta Astron., 20, 47

Paczyński B., Rudak B., 1980, A&A, 82, 349

Piersanti L., Cassisi S., Iben I. Jr., Tornambe A., ApJ, 535, 932

Pols O. R., Schröder K. P., Hurley J. R., Tout C. A., Eggleton P. P., 1998, MNRAS, 298, 525

Prialnik D., 1986, ApJ, 310, 222

Prialnik D., Kovetz A., 1995, ApJ, 445, 789

Reimers D., 1975, Mem.Soc.R.Sci.Liege, 8, 369

Seaquist E. R., Krogulec M., Taylor A. R., 1993, ApJ, 410, 260

Shima E., Matsuda T., Takeda H., Sawada K., 1985, MNRAS, 217, 235

Siess L., 2006, A&A, 448, 717

Soker N., Harpaz A., 2003, MNRAS, 343, 456

Sokoloski, J. L., et al. 2006, ApJ, 636, 1002

Somers M. W., Naylor T., 1999, A&A, 252, 563

Tauris T. M., Dewi J. D. M., 2001, A&A, 369, 170

Tout C.A., Eggleton P.P., 1988, MNRAS, 231, 823

Tutukov A.V., Yungelson L. R., 1976, Astrophysics, 12, 321

Uus U. H., 1970, Nauch. Inf., 17, 3

van Herk G., 1965, AN, 18, 71V

Vassiliadis E., Wood P. R., 1993, ApJ, 413, 641

Vogel M., 1991, A&A, 249, 173

Webbink, R. F. 1984, ApJ, 277, 355

Winters J. M., Le Bertre T., Jeong K. S., Helling Ch., Sedlmayr E., 2000, A&A, 361, 641

Winters J. M., Le Bertre T., Nyman L.-Å., Omont A., Jeong K. S., 2002 A&A, 388, 609

Winters J. M., Le Bertre T., Jeong K. S., Nyman L.-Å., Epchtein N., 2003, A&A, 409, 715

Woosley S.E., Weaver T.A., 1994, ApJ, 423, 371

Yaron O., Prialnik D., Kovetz A., 2005, ApJ, 623, 398

Yoon S. C., Langer N., 2004, A&A, 419, 645

Yungelson L., Tutukov A.V., 1993, in *Planetary Nebulae*, ed. R. Weinberger & A. Acker (Dordrecht: Kluwer), 389

Yungelson L., Livio M., Tutukov A. V., Saffer R. A., 1994, ApJ, 420, 336

Yungelson L., Livio M., Tutukov A. V., Kenyon S. J., 1995, ApJ, 477, 656, (YLTK)

Yungelson L., Livio M., Truran J. W., Fedorova A. X., 1996, ApJ, 466, 890

Yungelson L., Livio M., 1998, ApJ, 497, 168

This paper has been typeset from a *TeX/ L<sup>A</sup>T<sub>E</sub>X* file prepared by the author.